THESIS SUBMITTED IN PARTIAL FULFILMENT OF THE
REQUIREMENTS FOR THE DEGREE OF

MASTER OF SCIENCE

Charged Holographic Strings

Lior Blech

WRITTEN UNDER THE SUPERVISION OF
PROF. JACOB SONNENSCHEIN

September 11, 2016

Abstract

We revisit the holographic description of hadrons, adding an electromagnetic interaction term and taking account of one loop corrections through a casimir energy term. We first review the theoretical background: AdS/CFT correspondence, confining gravitational backgrounds and the approximating model of the spinning string with endpoint masses, including the one loop quantum corrections. We then analyse the effect of adding the electromagnetic charges and the casimir energy. Finally we confront the results with PDG data by fitting to the Regge trajectories and attempt to further constrict the parameter space through the determination of the mass difference between the up and down quarks.

Contents

1 Introduction

1.1 Confinement and Regge Trajectories

Confinement[3] is usually defined as the apparent absence of free quarks in nature. This definition refers to the absence of free hadronic particles with fractional electric charge. Although intuitive this definition is imprecise. Suppose in nature there exists a massive scalar in the fundamental representation of $SU(3)$ and otherwise no charge. This scalar and a quark would form a bound state in the trivial representation of $SU(3)$ and fractional electric charge, albeit with a higher mass, which could be detected at a future accelerator. This kind of particle would not really qualify as a free quark, but still, it motivates us to look for a better definition.

Another possible definition would be color confinement, which states that there are no isolated particles in nature with non vanishing color charge. This definition also does not capture the essence of the problem. Suppose we introduce a higgs field in the fundamental representation of $SU(3)$ with couplings such that all gluons acquire a mass at tree level. The color charge is the integral of the electric field over a closed volume:

$$Q^a = \int\limits_{\partial V} \vec{E}^a \cdot d\vec{S} \tag{1}$$

An isolated quark far from the boundary of the volume would thus have a color charge which is essentially zero, as the electric field would fall off exponentially with distance. So a quark viewed from a distance much greater than the inverse gluon mass would appear to be a color singlet.

What distinguishes a confining theory from a gauge theory with spontaneous symmetry breaking is the fact that meson states fall on Regge trajectories, which are not found in bound state systems with coulomb or yukawa attractive forces. Regge trajectories are straight lines in the (J, M^2) plane. It is well known that a linear quark interaction potential $V(r) = ar$ leads to linear Regge trajectories [4]. In gauge theories the operators called Wilson lines (or loops) are gauge invariant operators defined by

$$W(C) = \frac{1}{N} TrPe^{\,i \oint\limits_C A_\mu \dot{x}^\mu(\tau) \mathrm{d}\tau} \tag{2}$$

The interaction potential of a quark anti-quark pair can be extracted from the infinite strip Wilson line by the relation [12]:

$$\langle W(C) \rangle = A(L)\, e^{-TE(L)} \tag{3}$$
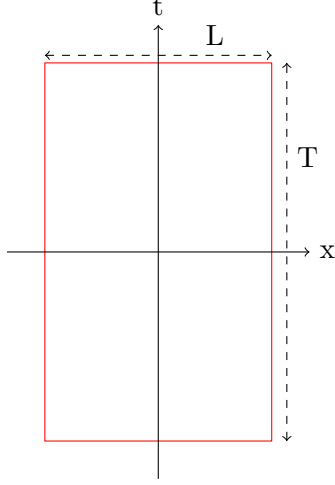
Where T is the time extension of the loop. Assuming the interaction potential is linear we get that the Wilson line has an area law behaviour

$$\langle W\left(C\right)\rangle = A\left(L\right)e^{-aTL} \tag{4}$$

This is why an area law for the Wilson line is considered as a signal for a confining theory.

A simple model which was already known in the 60s [1] to replicate the linear nature of Regge trajectories, is the spinning open relativistic string given by the Namboo-Goto action. The NG action describes the proper area of the string worldsheet:

$$S = T_{string}\iint \mathrm{d}^2\sigma\sqrt{-\det\left(\frac{\partial x^\mu}{\partial\sigma^a}\frac{\partial x_\mu}{\partial\sigma^b}\right)} \tag{5}$$

Where $T_{string}\left[GeV^{-2}\right]$ is the string tension and

$$\sigma^1 = \tau \in (-\infty,\infty) \tag{6}$$
$$\sigma^2 = \sigma \in [-\pi,\pi] \tag{7}$$

Are the worldsheet coordinates, which are affine parameters describing the worldsheet. The action is invariant upon general coordinate transformations. We choose in this case the orthogonal gauge which is defined by:

$$\frac{dx^\mu}{d\tau}\frac{dx_\mu}{d\tau} = -\frac{dx^\mu}{d\sigma}\frac{dx_\mu}{d\sigma} \tag{8a}$$

$$\frac{dx^\mu}{d\sigma}\frac{dx_\mu}{d\tau} = 0 \tag{8b}$$

Under which the action reduces to the more convenient form:

$$S = \frac{T_{string}}{2}\iint\left(\frac{dx^\mu}{d\tau}\frac{dx_\mu}{d\tau} - \frac{dx^\mu}{d\sigma}\frac{dx_\mu}{d\sigma}\right)\mathrm{d}\sigma\mathrm{d}\tau \tag{9}$$

4

The conjugate momenta are:

$$P^\mu = \frac{\partial \mathcal{L}}{\partial \dot{x}^\mu} = T_{string}\eta_{\mu\nu}\dot{x}^\nu \tag{10}$$

The boundary conditions appropriate for an open string are:

$$\dot{x}^0_{\sigma=\pm\pi} = const \tag{11a}$$

$$P^i_{\sigma=\pm\pi} = 0 \tag{11b}$$

And the equations of motion are simply the wave equation for each coordinate:

$$\frac{\partial^2 x^\mu}{\partial \tau^2} - \frac{\partial^2 x^\mu}{\partial \sigma^2} = 0 \tag{12}$$

A solution describing a spinning string is:

$$x^0 = A\tau \qquad\qquad x^3 = \cdots = const$$

$$x^1 = A\cos(\tau)\sin(\sigma) \qquad\qquad x^2 = A\sin(\tau)\sin(\sigma) \tag{13}$$

The parameter A is needed in the time variable to ensure the solution is in the orthogonal gauge. We now compute the energy and angular momentum of this configuration and find the relation in the (J, E^2) plane. The energy is the generator of poincare time translations and angular momentum is the generator of rotations in the poincare coordinates. The expressions are:

$$E = \frac{T_{string}}{2} \int\limits_{-\pi}^{\pi} \frac{dx^0}{d\tau} \mathrm{d}\sigma \tag{14a}$$

$$J_i = \frac{T_{string}}{2} \int\limits_{-\pi}^{\pi} \epsilon_{ijk}x_j\dot{x}^k \mathrm{d}\sigma \tag{14b}$$

Substituting the spinning solution into these results in:

$$E = \pi T_{string}A \tag{15a}$$

$$J_3 = \frac{T_{string}\pi}{2}A^2 \tag{15b}$$

Finally we combine the two relations, eliminating A in favour of E in J and get the formula for a classical linear trajectory:

$$J = \frac{E^2}{2\pi T_{string}} \tag{16}$$

Here we can define a quantity which we will use later, the Regge slope $\alpha' = \frac{1}{2\pi T_{string}}$. The expression 16 lacks another important property of Regge

trajectories: the *intercept*. The intercept is the result of quantum mechanical fluctuations, as will be demonstrated in section 1.4. Due to this interesting result string theory was initially investigated as a theory of the strong interactions. Due to the presence of unwanted (from the strong interaction point of view) particles in the string spectrum and the discovery of asymptotic freedom, it was abandoned as a theory of the strong interactions, while continuing to develop as a fundamental theory of particle physics and gravity.

1.2   The AdS/CFT Correspondence

In time it was discovered that apart from strings, string theory contained additional degrees of freedom, p-Branes, which are extended objects where open strings end. Furthermore, p-Branes were recognized to be the same objects as D Branes, which are solitonic solutions of supergravity (which is the low energy, or small slope, limit of superstring theory). Dp Branes, as they are called, can also carry gauge fields which are said to "live" on their surface. Open strings then correspond to sources or sinks of flux on the brane.

The study of Dp Branes and the theories that live on them led to the Maldacena conjecture that $\mathcal{N} = 4$ SYM is equivalent to type IIB string theory compacted on $AdS_5 \times S^5$[5, 8, 9]. The conjecture relates the string theory, supergravity and gauge theory parameters:

$$g_{YM}^2 \equiv \frac{\lambda}{N} = 4\pi g_s \qquad\qquad R_{S_5}^2 = R_{AdS_5}^2 = \lambda^{1/2}\alpha' \qquad (17)$$

Where

g_{YM} is the gauge theory coupling

λ is the t'Hooft coupling

N is the number of coincident D Branes as well as the type of gauge group $SU(N)$

g_s is the string coupling

R_{S_5} is the radius of the sphere

R_{AdS_5} is the radius of AdS

α' is the slope parameter as defined above

The SYM theory lives on the boundary of AdS while the string theory lives in the bulk. The perturbative description is valid for small g_{YM} while the supergravity description is valid for large radii, hence large λ and finite g_{YM}. In this sense it is also a weak-strong coupling correspondence. A consequence of the correspondence must be that correlation functions in

the gauge theory can be computed in the string theory by using the gauge theory operator insertions as the boundary conditions for the string theory computations. The correspondence in the generating functional is:

$$Z_{SYM}(\theta_0) = <e^{\int d^4 x \theta_0(x) Q(x)}> \sim Z_{stringy}(\theta_0) = \int\limits_{\theta \to \theta_0} \mathcal{D}\theta e^{-S[\theta]} \qquad (18)$$

Where $\theta_0(x)$ is the source of the boundary field $Q(x)$.

SYM theory is a supersymmetric version of Yang Mills theory, which turns out to be conformally invariant at the quantum level. The most powerful evidence for the AdS/CFT correspondence is the correspondence of $SYM \mathcal{N} = 4$ theory to string theory on the $AdS_5 \times S_5$ background. The correspondence in this case is supported by the fact that the two theories contain the same symmetries. We will now briefly describe conformal symmetry ,supersymmetry and the symmetries of AdS space.

The Conformal symmetry group is the group of transformations which preserve the form of the metric up to an arbitrary scale factor $g_{\mu\nu}(x) \to \Omega^2(x) g_{\mu\nu}(x)$. It is generated by the poincare transformations, the scale transformations

$$x^\mu \to \lambda x^\mu \qquad (19)$$

and the special conformal transformations

$$x^\mu \to \frac{x^\mu + a^\mu x^2}{1 + 2x^\nu a_\nu + a^2 x^2} \qquad (20)$$

The generators of Lorentz $M_{\mu\nu}$, Translation P_μ, Scale D and Special Conformal K_μ transformations obey the conformal algebra:

$$[M_{\mu\nu}, P_\rho] = -i(\eta_{\mu\rho} P_\nu - \eta_{\nu\rho} P_\mu) \qquad [M_{\mu\nu}, K_\rho] = -i(\eta_{\mu\rho} K_\nu - \eta_{\nu\rho} K_\mu)$$
$$[M_{\mu\nu}, M_{\rho\sigma}] = -i\eta_{\mu\rho} M_{\nu\sigma} \pm permutations \qquad\qquad [D, K_\mu] = iK_\mu$$
$$[D, P_\mu] = -iP_\mu \qquad\qquad [P_\mu, K_\nu] = 2iM_{\mu\nu} - 2i\eta_{\mu\nu}D$$
$$[M_{\mu\nu}, D] = 0 \qquad (21)$$

where all other commutators vanish. This algebra is isomorphic to the algebra of $SO(d,2)$ with signature $-, +, +, \ldots, +, -$ and generators J_{ab}:

$$J_{\mu\nu} = M_{\mu\nu} \qquad J_{\mu d} = \frac{1}{2}(K_\mu - P_\mu) J_{\mu(d+1)} = \frac{1}{2}(K_\mu + P_\mu) \quad J_{(d+1)d} = D \qquad (22)$$

$\mu, \nu = 0, 1, \ldots, d-1$

The supersymmetry transformation is generated by a fermionic operators Q which anti-commutes with the translation operators P_μ. For some numbers of dimensions and supersymmetry generators it is possible to join

the supersymmetry and conformal group into one simple group. These superconformal algebras exist only for $d \leq 6$. In these algebras there arise two more types of generators: the fermionic S and the bosonic R R-symmetry. The algebra is schematically:

$$[D, Q] = -\frac{i}{2}Q \qquad [D, S] = \frac{i}{2}S[K, Q] \approx S \qquad\qquad [P, S] \approx Q$$

$$Q, Q \approx P \qquad\qquad S, S \approx KQ, S \approx M + D + R \qquad\qquad (23)$$

The $p + 2$ dimensional Ads_{p+2} can be represented as the hyperboloid

$$X_0^2 + X_{p+2}^2 - \sum_{i=1}^{p+1} X_i^2 = R^2 \qquad\qquad (24)$$

in the flat $p + 3$ dimensional space with metric

$$ds^2 = -dX_0^2 - dX_{p+2}^2 + \sum_{i=1}^{p+1} dX_i^2 \qquad\qquad (25)$$

This space has the isometry $SO(2, p + 1)$ by construction and it is homogeneous and isotropic. A useful set of coordinates $(u, t, \vec{x})$, called the poincare coordinates, is defined by the relations:

$$X_0 = \frac{1}{2u}\left(1 + u^2\left(R^2 + \vec{x}^2 - t^2\right)\right) \qquad\qquad X_{p+2} = Rut$$

$$X^i = Rux^i \qquad (i = 1, \ldots, p)$$

$$X^{p+1} = \frac{1}{2u}\left(1 - u^2\left(R^2 - \vec{x}^2 + t^2\right)\right) \qquad\qquad (26)$$

In these coordinates the metric is:

$$ds^2 = R^2\left(\frac{du^2}{u^2} + u^2\left(-dt^2 + d\vec{x}^2\right)\right) \qquad\qquad (27)$$

The metric is manifestly poincare invariant ($ISO\,(1, p)$). Also the transformation $SO\,(1, 1)$ defined by:

$$(t, \vec{x}, u) \rightarrow \left(ct, c\vec{x}, c^{-1}u\right) \qquad c > 0 \qquad\qquad (28)$$

is an isometry of the space. This transformation is identified with the dilatation D in the conformal symmetry group of $\mathbb{R}^{1,p}$. Thus AdS_{p+2} has the same number of symmetries as a conformal theory in flat space with $p + 1$ dimensions.

Lastly the $SO\,(2, p + 1)$ isometry group of AdS_{p+2} has a supersymmetric generalization called an AdS supergroup, and it turns out that AdS space preserves as many supersymmetries as flat space.

The exact matching between the superconformal algebra of $SYM\,\mathcal{N} = 4$ and the isometry group of supergravity (and thus low energy string theory) on $AdS_5 \times S_5$ provides the strongest evidence for the maldacena correspondence.

1.3 Confining Backgrounds

As has been mentioned, the Maldacena correspondence allows us to compute strong coupling quantities in gauge theories. This has given hope that a string theory dual to QCD might be found which would enable us to handle the nonperturbative regime. The fact that string models describe well the Regge trajectories gives further motivation. While this has not been accomplished to date, there has been progress in that direction.

Using the gauge-gravity duality, supergravity backgrounds have been constructed that are dual to confining gauge theories. To deal with non supersymmetric gauge dynamics one makes use of Witten's method [6, 7] of using compact euclidean time with anti-periodic boundary conditions. We investigate whether the stringy picture in a confining background can reproduce the properties of real hadrons by fitting to regge trajectories and predict hadron electromagnetic mass differences. This section summarizes the results of previous works on what kinds of backgrounds confine.

1.3.1 The Stringy Wilson Line

In the AdS/CFT correspondence, the stringy dual of the Wilson line is the Nambu-Goto string [10].

$$\langle W\left(C\right)\rangle \sim e^{-S_{NG}} \tag{29}$$

So that

$$S_{NG} = TE\left(L\right) \tag{30}$$

We analyse a Wilson line inside a d dimensional space-time with the metric [20]

$$ds^2 = -G_{00}\left(s\right)dt^2 + G_{||}\left(s\right)dx_{||}^2 + G_{ss}\left(s\right)ds^2 + G_{TT}\left(s\right)dx_T^2 \tag{31}$$

where the $x_{||}$ are p space coordinates on a D_p brane and **s** and x_T are radial coordinates and transverse directions respectively. For string configurations which are static and approximately stretch only along the radial and one $x_{||}$ directions we can take the gauge $t = \tau, x_{||} = x$. The induced worldsheet metric then takes the form:

$$h = \begin{pmatrix} -G_{00} & 0 \\ 0 & G_{||} + G_{ss}\left(\partial_x s\right) \end{pmatrix} \tag{32}$$

The corresponding Nambu Goto action is

$$S_{NG} = T\int \sqrt{f^2\left(s\left(x\right)\right) + g^2\left(s\left(x\right)\right)\left(\partial_x s\right)^2}dx \tag{33}$$

Where $T = \int dt$ and we made the following substitutions:

$$f^2\left(s\left(x\right)\right) = G_{00}\left(s\left(x\right)\right)G_{||}\left(s\left(x\right)\right) \tag{34a}$$

$$g^2\left(s\left(x\right)\right) = G_{00}\left(s\left(x\right)\right)G_{ss}\left(s\left(x\right)\right) \tag{34b}$$

Notice that $\mathbf{x}$ does not appear explicitly in the action and so there is a conserved current:

$$\frac{\partial L_{NG}}{\partial (ds/dx)} \frac{ds}{dx} - L_{NG} = const$$

$$= \cdots = -\frac{f^2 (s(x))}{\sqrt{f^2 (s(x)) + g^2 (s(x)) (\partial_x s)^2}} = const = -K \qquad (35)$$

For $\frac{ds}{dx}|_{s_0} = 0$ we get $f(s_0) = K$. Using this and extracting $\frac{ds}{dx}$ we get:

$$\frac{ds}{dx} = \pm \frac{f(s)}{g(s)} \frac{\sqrt{f^2(s) - f^2(s_0)}}{f(s_0)} \qquad (36)$$

The picture is of the string stretching down from the boundary $s \to \infty$ down to $s \to s_0$ where it is horizontal, and back into the boundary. The separation distance between the string endpoints (quark anti quark) is

$$L = \int dx = 2 \int\limits_{s_0}^{\infty} \frac{g(s)}{f(s)} \frac{f(s_0)}{\sqrt{f^2(s) - f^2(s_0)}} ds \qquad (37)$$

We can use the two relations to calculate the action and extract the quark potential $E = \frac{S_{NG}}{T}$

$$S_{NG} = 2T \int\limits_{s_0}^{\infty} \frac{g(s)}{f(s)} \frac{f(s_0)}{\sqrt{f(s)^2 - f(s_0)^2}} \sqrt{f(s)^2 + g(s)^2 \frac{f(s)^2}{g(s)^2} \frac{f(s)^2 - f(s_0)^2}{f(s_0)^2}} ds$$

$$= 2T \int\limits_{s_0}^{\infty} \frac{g(s) f(s)}{\sqrt{f(s)^2 - f(s_0)^2}} ds = \infty \qquad (38)$$

The action diverges because of the infinite extent of the string. In order for the string length to converge the slope $\frac{ds}{dx}$ has to diverge on the boundary. This implies $f(s) \gg f(s_0)$ on the boundary. In this region the string is vertical and the energy density there is approximately just $g(s)$. In that case we can renormalize the action by

(a) regularizing the integral $\int\limits_{s_0}^{\infty} \to \int\limits_{s_0}^{s_1}$

(b) substracting the quark masses defined by

$$m_q = \int\limits_0^{s_1} g(s) \, ds \qquad (39)$$

10

The renormalized quark antiquark potential is now

$$V = f\left(s_0\right)L + 2\int\limits_{s_0}^{s_1}\frac{g\left(s\right)}{f\left(s\right)}\left(\sqrt{f\left(s\right)^2 - f\left(s_0\right)^2} - f\left(s\right)\right)\mathrm{d}s - 2\int\limits_{0}^{s_0}g\left(s\right)\mathrm{d}s \quad (40)$$

A sufficient condition for confinement found in [12, 19] is if either:

- f has a minimum at s_{min} and $f\left(s_{min}\right) \neq 0$.

- g diverges at s_{div} and $f\left(s_{div}\right) > 0$.

The first condition asserts that the potential contains a linear term. Also under this condition there must be a region where $f\left(s\right) \gg f\left(s_0\right)$. In the case of a divergence of $g\left(s\right)$,

$$\frac{ds}{dx}|_{s=s_{div}} = \pm\frac{f\left(s\right)}{g\left(s_{div}\right)}\frac{\sqrt{f^2\left(s\right) - f^2\left(s_0\right)}}{f\left(s_0\right)} = 0 \quad (41)$$

So that a string long enough to reach s_{div} stretches horizontally along $s = s_{div}$ for much of its length. So the stringy picture in a confining background is that of two strings stretching vertically from the boundary down to either the "wall" $s = s_{div}$ or down to s_0 where f has a minimum, and connecting horizontally.

An example is that of the dual model of pure YM in d=3 [19]:

$$L_{NG} = \sqrt{\left(\frac{U}{R}\right)^4 + \left(U'\right)^2\left(1 - \left(\frac{U_T}{U}\right)^4\right)^{-1}} \quad (42a)$$

$$V = \frac{U_T^2}{2\pi R^2}L - 2\kappa + O\left(\left(\log L\right)^{\beta}e^{-\alpha L}\right) \quad (42b)$$

This has confining behaviour and $S_{div} = U_T$. In other words to get confinement we introduce a scale in the radial direction. The Wilson line in a confining background behaves similarly to a string in flat space time, due to the U shape and the cancellation of the action of the vertical segments.
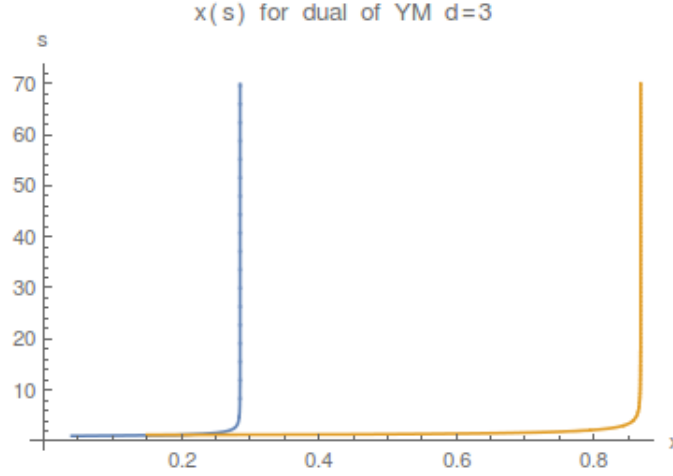
Figure 1: String configurations of the YM dual 42 with $s_{div} = R = 1$. The blue and orange strings differ in the overall string length, controlled through the dependence on s_0 37. It can be observed that the length of the transition region between horizontal and vertical sections does not scale with the string length.

1.3.2   From Wilson Lines To Dynamical Mesons

In the preceding section we discussed the stringy description of the Wilson line. The quarks there were actually infinitely massive due to the strings stretching all the way to the boundary. We can introduce dynamical quarks by introducing a set of N_f "flavour" Dp Branes in the bulk, in addition to the stack of (N_c) "color" branes which lie at the boundary. Strings which stretch between the color branes and the flavour branes map to bi-fundamental "quarks" that transform as the (N_c, N_f) representation of the $U(N_c) \times U(N_f)$ gauge symmetry. For $N_c \gg N_f$ the back reaction of the flavour branes can be ignored and the $U(N_f)$ can be treated as a global symmetry.

We use the Sakai-Sugimoto model [25] which consists of N_c D4 branes and N_f $D8 - D\bar{8}$ branes. The dimensions the branes extend along are described in table 1. The x^4 coordinate is compacted with boundary conditions which kill supersymmetry and introduces confinement. The flavour

	0	1	2	3	(4)	5	6	7	8	9
$D4$	○	○	○	○	○					
$D8 - D\bar{8}$	○	○	○	○		○	○	○	○	○

Table 1: The Sakai-Sugimoto model brane configuration. The dimension x^4 is compacted on a circle.
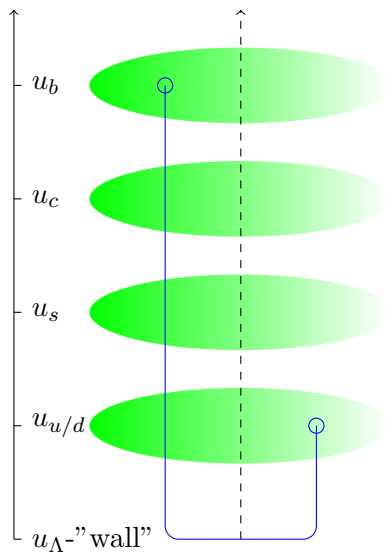
Figure 2: Illustration of flavour probe branes. Each brane is located at a different radial coordinate which determines the mass of the corresponding quark flavour.

branes in the $D4$ background are described by the embedding $x^4(U)$ where U is the radial direction away from the $D4$ brane (with the $D4$ brane residing at $U = \infty$). In their analysis Sakai and Sugimoto determined that the $D8 - D\bar{8}$ branes hang from the $D4$ brane and meet at some U, forming a single brane and spontaneously breaking the chiral symmetry $U(N_f)_L \times U(N_f)_R \to U(N_f)$. One can separate the flavour branes in the radial U direction, further breaking the flavour symmetry.

Now instead of starting and ending on the boundary the strings can start and end on the flavour branes. A string would now have an endpoint mass:

$$m_q = T \int\limits_{s_0}^{s_f} \sqrt{G_{00} G_{ss}} \, \mathrm{d}s \tag{43}$$

Where s_f is the radial coordinate of a flavour brane. In [21] it was found that the dynamics of the open string spinning in the confining background could be described by the model of the spinning string in flat space loaded with masses at its' ends. This approximation is valid as long as the string is sufficiently long and stretches along the wall.

We have seen that it is possible to get a string theory which is dual to a confining gauge theory with flavour symmetries and fundamental quarks and the states dual to mesons are spinning strings stretching between the flavour branes. In [26] a similar analysis was carried out for baryons, which were found to be described by spinning strings which at one end connect

with a flavour brane and at the other end with a baryonic vertex, which then connects with two other short strings which in turn connect to flavour branes. The baryonic vertex is itself a D5 brane wrapped around the S_5. In addition we see that this theory can be analysed through the approximation of the spinning string with masses at the endpoints. This approximation lies at the heart of the present work.

1.4 Spinning Holographic Strings

In the previous section we have seen that strings in gravitational backgrounds which connect with probe branes can be approximately described as strings in flat space-time, with endpoint masses proportional to the length of the horizontal string sections. This section will present the results obtained in the analysis of such a model and use them to discuss the general approach to the holographic string problem.

The model of the spinning string with massive endpoints is described using the Nambu-Goto action and relativistic point particle action:

$$
S = -T \int\int_{(0,-l_2)}^{(T,l_1)} \mathrm{d}^2\sigma \sqrt{-\det h} - m_1 \int_0^T \mathrm{d}\tau \sqrt{u^\mu u_\mu}|^{\sigma=l_1} - m_2 \int_0^T \mathrm{d}\tau \sqrt{u^\mu u_\mu}|^{\sigma=-l_2} =
$$

$$
= -T \int\int_{(0,-l_2)}^{(T,l_1)} \mathrm{d}^2\sigma \sqrt{-\det h} - m \int_0^T \mathrm{d}\tau \sqrt{u^\mu u_\mu}|_{\sigma=-l_2}^{\sigma=l_1} \tag{44}
$$

The endpoint masses (point like massive particles) are located at the coordinates specified by $\sigma = l_1, -l_2$, and the masses are allowed to vary between the two ends. The second line of equation 44 shows an example of a shorthand we use to write the two point-particle actions as one.

In section 2.4 we show how to derive the equations of motion, energy and angular momentum for the case of the charged holographic string discussed there. For now we simply write down the results obtained in [13] for the case of identical endpoint masses.

14

The equation of motion is:

$$\gamma\beta m\omega - \frac{T}{\gamma} = 0 \tag{45a}$$

The energy is:

$$E = \frac{2T}{\omega}\sin^{-1}(\beta) + 2m\gamma \tag{45b}$$

The angular momentum is:

$$J = T\frac{-\frac{\beta}{\gamma} + \sin^{-1}(\beta)}{\omega^2} + 2m\frac{\gamma\beta^2}{\omega} \tag{45c}$$

Where:

c = 1.

β is the velocity of the endpoints.

$\gamma = \frac{1}{\sqrt{1-\beta^2}}$

T is the string tension.

ω is the rate of rotation, such that $\beta = \omega l$ and l is the distance of each endpoint to the center of rotation.

Notice that the equation of motion can be used to relate the rate of rotation with the velocity:

$$\omega = \frac{T}{m\gamma^2\beta} \tag{46}$$

So putting this back in the expressions for the energy and angular momentum results in:

$$E = 2m\gamma^2\beta\sin^{-1}(\beta) + 2m\gamma \tag{47a}$$

$$J = m^2\gamma^4\beta^2\frac{-\frac{\beta}{\gamma} + \sin^{-1}(\beta)}{T} + \frac{2m^2\gamma^3\beta^3}{T} \tag{47b}$$

We are interested in the predicted regge trajectories in the limits of small and large quark mass, which corresponds to $\beta \to 1$ and $\beta \to 0$ respectively (this results from equation 46, assuming constant string tension and rotation rate).The procedure to get the expression for the regge trajectory in each limit is:

1. Expand the energy and angular momentum in a Taylor series around the corresponding limit.

2. Find the inverse series for the energy $\beta(E)$ [2].

3. Plug $\beta(E)$ into the angular momentum series and get $J(E)$.

The resulting series are:

Light quark limit $\beta \to 1$

$$J = \alpha'E^2 - \frac{8\sqrt{\pi}\alpha'm^{3/2}}{3}\sqrt{E} + \frac{2}{5}\frac{\pi^{3/2}m^{5/2}\alpha'}{\sqrt{E}} + \dots \qquad (48a)$$

Heavy quark limit $\beta \to 0$

$$J = \frac{4\pi\alpha'\sqrt{m}\,(E-2m)^{3/2}}{3\sqrt{3}} + \frac{7\pi\alpha'\,(E-2m)^{5/2}}{54\sqrt{3}\sqrt{m}} + \dots \qquad (48b)$$

Here we have defined the string 'slope' related to the string tension by:

$$\alpha' = \frac{1}{2\pi T} \qquad (49)$$

Observe that in the light quark limit the regge trajectory reduces to the linear trajectory of the spinning string with no endpoint masses $J = \alpha'E^2$.

1.5   Quantization of the String with Massive Ends

The trajectory in the last section still does not predict an intercept. The intercept is created by the quantum mechanical zero point energy. This energy is also called a casimir energy because in the casimir effect it is the energy difference induced by this energy term which causes the observed casimir force. It is well known that the intercept is given in terms of the casimir term which is the sum of the eigenvalues of the world sheet Hamiltonian ω_n:

$$E_{casimir} = \frac{1}{2}\sum_{n=1}^{\infty}\omega_n = \frac{\pi(D-2)}{2L}\sum_{n=1}^{\infty}n = -\frac{(D-2)}{24}\frac{\pi}{L} = a\frac{\pi}{L} \qquad (50)$$

where $\omega_n = n$ for the case of the open string with Dirichlet boundary conditions and a zeta function regularization has been performed. Our case differs however in two ways:

- Our model lives in four dimensions, which is not the critical dimension of the bosonic string.

- Our model contains a rotating string with massive endpoints instead of a string with Dirichlet boundary conditions.

The question of quantizing the string in non-critical dimensions was addressed by Polyakov and more recently in [15][16][17]. The basic observation

is that for the quantum effective string action in D dimensions, it is necessary to add a Liouville term of the form:

$$S_L = \frac{26 - D}{24\pi} \int d^2\sigma \sqrt{|g|} \left[g^{ab} \partial_a \varphi \partial_b \varphi - \mathcal{R}_2 \varphi \right] \tag{51}$$

where the Liouville field is a composite field of the form

$$\varphi = -\frac{1}{2} Log(g^{ab} \partial_a x^\mu \partial_b x_\mu) \tag{52}$$

An alternative formulation for the non-critical string was proposed by Polchinski-Strominger in [15]. In the orthogonal gauge it reads:

$$S_{PS} = \frac{26 - D}{24\pi} \int d\theta \int_{-\delta}^{\delta} d\sigma \frac{\left(\partial_+^2 X \cdot \partial_- X \right) \left(\partial_+ X \cdot \partial_-^2 X \right)}{\left(\partial_+ X \cdot \partial_- X \right)^2} \tag{53}$$

Both formulations result in the same contribution to the action and have to be added to the open string as well as the closed string with either massless of massive end points. The purpose of the Polchinski-Strominger term (as in the case of the Liouville term) is to restore 2d conformal invariance for the non-critical string. Although it looks somewhat arbitrary at first sight, this term naturally appears in the Wilsonian quantization of the effective string in non-critical dimension and so is an integral part of the effective string action.

In [18] the quantum corrections to the energy of the massive stationary string have been calculated. There it can be seen that the Hamiltonian for the stationary string is reduced to:

$$H = \sum_{n=1}^{\infty} \sum_{j=1}^{D-2} \omega_n a_n^{j\dagger} a_n^j + TR + \frac{D-2}{2} \sum_{n=1}^{\infty} \omega_n + \sum_{i=1,2} m_i \tag{54}$$

Where the eigenfrequencies ω_n satisfy:

$$\tan(\omega_n R) = \frac{2mTR(\omega_n R)}{m^2 \omega_n^2 R^2 - T^2 R^2} \tag{55}$$

Where R is the string length and D is the number of space-time dimensions, so that the energy in terms of the dimensionless quantity $\Omega_n = \omega_n R$ is:

$$H = \frac{1}{R} \sum_{n=1}^{\infty} \sum_{j=1}^{D-2} \Omega_n a_n^{j\dagger} a_n^j + TR + \frac{D-2}{2R} \sum_{n=1}^{\infty} \Omega_n + \sum_{i=1,2} m_i \tag{56}$$

Therefore the string potential is

$$V(R) = TR + \frac{D-2}{2R} \sum_{n=1}^{\infty} \Omega_n \tag{57}$$

Note that in the limits of infinite and zero mass $\Omega_n = n$ and the result of the string with massless ends is recovered. The casimir term calculated in [18] is plotted in figure 3, where

$$\eta(q) = \frac{E_C^{ren}(m, L)}{E_C^{ren}(m = \infty, L)} = -\frac{12}{\pi^2} \int_0^\infty dx Lan \left[1 - e^{-2x} \left(\frac{q - x}{q + x} \right)^2 \right] \quad (58)$$

and the definition of q is the ratio of the string length L, tension T and endpoint mass m:
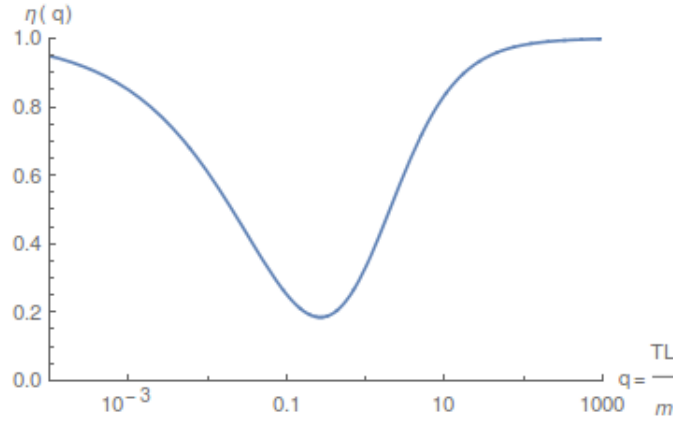
$$q = \frac{TL}{m} \quad (59)$$

Figure 3: Plot of casimir term value as a function of tension, string length and endpoint mass in the case of the stationary string. Taken from [18]

So we see that the string introduces both a confining linear potential and a $1/R$ term. This term is the generalization of the famous Luscher term. In the case of the string with massive endpoints it turns out this additional potential is attractive, similar to the Luscher result, but has mass and string length dependent corrections. This leads us to guess that the quantum correction to the spinning holographic string can be made by introducing a casimir energy term of the same form with some free parameter which stands in for the sum $\sum_{n=1}^\infty \Omega_n$.

In [13] the charges of the quarks have not been taken account of. The charges are expected to contribute to observables such as the mass differences between different hadrons, as well as decay rates and magnetic and electric dipoles. In the next section we will add the point charges and take the same philosophy: calculate the classical trajectory and add the quantum corrections by hand (although a bit differently).

In previous work on the holographic string[13] the intercept has been introduced by taking

$$J \rightarrow J - a \quad (60)$$

18

1.6 Potential Models

Before going into the specifics of our model, it is worth mentioning another approach available for probing the low energy dynamics of QCD. The approach of non-relativistic potential models [4] postulates that the binding force inaccessible to perturbation theory can be written as a non-relativistic potential, commonly:

$$V_{confining}(r) = a \cdot r^n \qquad 2 > n > 0, a > 0 \tag{61}$$

The exponent of r is designed to be a long distance interaction ($n > 0$ so that the force does not decrease faster than $\frac{1}{r}$), while not inducing equidistant level spacings (as in the case of the harmonic oscillator, $n = 2$). A choice of $n = 1$ is conventional and when combined with relativistic dynamics reproduces the Regge Trajectories. By considering the elastic scattering of quarks, the short distance part of the potential can be derived from QCD perturbation theory in the following way:

- Compute the scattering amplitude T_{fi} in lowest non-trivial order of perturbation theory

- Perform the non-relativistic limit

- obtain the potential $V(r)$ in the born approximation as the Fourier transform

$$V(r) = -(2\pi)^3 \int d^3k e^{-ik \cdot r} T_{fi}(k) \tag{62}$$

For example the quark forces within a meson can be derived from quark-anti-quark scattering and leads to

$$V(r) = -\frac{4}{3}\alpha_s/r \qquad \text{with} \qquad \alpha_s \equiv g_s^2/4\pi \tag{63}$$

while the quark forces within a baryon are derived from quark-quark scattering and yields

$$V(r) = -\frac{2}{3}\alpha_s/r \tag{64}$$

Combining the short distance and large distance potentials results in the so called "funnel potential" (in the case of mesons):

$$V(r) = -\frac{4}{3}\alpha_s/r + ar + V_0 \tag{65}$$

One then uses this potential in the time independent schrodinger equation and calculates the energies and wavefunctions for hadrons. It has also been shown within the potential models formalism that when combined with relativistic kinematics, a linear potential leads to linear Regge trajectories.

Further details, like spin orbit interactions and relativistic corrections can be found in the reviews on the subject, i.e. [4]. Our interest in the subject is due to the fact that within this formalism it is possible to calculate the matrix elements corresponding to the electric dipole of the hadron $\langle \psi_f | q(\vec{r}) \vec{r} | \psi_i \rangle$, which should be used to calculate the width of the hadron due to radiating electromagnetically.

2 Charged Holographic Strings

The strings in our model attach to stacks of N_f flavour branes. As such they are charged under the gauge group $SU(N_f)$. If the flavour branes are separated this gauge group gets broken spontaneously down to a number of $U(1)$ gauge groups, which is just the electromagnetic interaction. In our model we take account of the electromagnetic interaction by associating electric charge with the string endpoints. We now present the formulation and analyse the model.

2.1 The Action

We add charges to the end points by considering the action from the previous section and adding two electromagnetic interaction lagrangians at the endpoints. Note that instead of using the Namboo-Goto action for the string one can use the polyakov action, and similarly the point particles can be described by the alternative action quadratic in the coordinates. We use here the choice of a Namboo Goto action for the string and a "proper interval" action for the point masses:

$$
S = -T \int\!\!\!\int_{(0,-l_2)}^{(T,l_1)} \mathrm{d}^2\sigma \sqrt{-\det h} - m \int_0^T \mathrm{d}\tau \sqrt{u^\mu u_\mu}\big|_{\sigma=-l_2}^{\sigma=l_1} - q \int_0^T u^\mu A_\mu \mathrm{d}\tau\big|_{\sigma=-l_2}^{\sigma=l_1} \quad (66)
$$

The field lagrangian density for the electromagnetic fields is not included to avoid divergent self energy terms .Instead, the electromagnetic potentials and fields are determined directly by the Lienard-Wichert formulas. The worldsheet metric is as usual:

$$
h = \begin{pmatrix} \frac{dx^\mu}{d\tau}\frac{dx_\mu}{d\tau} & \frac{dx^\mu}{d\tau}\frac{dx_\mu}{d\sigma} \\ \frac{dx^\mu}{d\tau}\frac{dx_\mu}{d\sigma} & \frac{dx^\mu}{d\sigma}\frac{dx_\mu}{d\sigma} \end{pmatrix}
$$

We can write for short

$$
V^\mu = \frac{dx^\mu}{d\sigma} \qquad\qquad u^\mu = \frac{dx^\mu}{d\tau}
$$

$$
h = \begin{pmatrix} u^2 & u \cdot V \\ u \cdot V & V^2 \end{pmatrix}
$$

The action can be written then as:

$$S = -T \int\!\!\!\int_{(0,-l_2)}^{(T,l_1)} \mathrm{d}^2\sigma \sqrt{(u \cdot V)^2 - u^2 V^2} - m \int_0^T \mathrm{d}\tau \sqrt{u^\mu u_\mu}|_{\sigma=-l_2}^{\sigma=l_1} - q \int_0^T u^\mu A_\mu \mathrm{d}\tau|_{\sigma=-l_2}^{\sigma=l_1}$$

(67)

We use the static gauge where:

$$t = \tau \qquad r = \sigma$$ (68)

The 4 velocity in this gauge is

$$u^\mu = \left(\frac{dt}{d\tau}, \frac{dx}{d\tau}, \frac{dy}{d\tau}, \frac{dz}{d\tau} \right) = \left(1, \sigma \frac{d\cos(\theta)}{d\tau}, \sigma \frac{d\sin(\theta)}{d\tau}, 0 \right) =$$
$$= \left(1, -\sigma\dot\theta\sin(\theta), \sigma\dot\theta\cos(\theta), 0 \right)$$

The basis vectors for polar coordinates are

$$\hat{r} = \frac{1}{r}(x\hat{x} + y\hat{y}) \qquad\qquad \hat{\theta} = \frac{1}{r}(x\hat{y} - y\hat{x})$$

The components for A^μ in polar coordinates are thus:

$$A^r = \vec{A} \cdot \hat{r} = \frac{xA^x + yA^y}{\sigma} = cos(\theta) A^x + sin(\theta) A^y$$

$$A^\theta = \vec{A} \cdot \hat{\theta} = \frac{-yA^x + xA^y}{\sigma} = -sin(\theta) A^x + cos(\theta) A^y$$

Which can be recognized as a rotation by angle θ. The inverse transformation is then:

$$A^x = cos(\theta) A^r - sin(\theta) A^\theta$$
$$A^y = sin(\theta) A^r + cos(\theta) A^\theta$$

The product-sum $u^\mu A_\mu$ in our gauge is then:

$$u^\mu A_\mu = u^t A^t - u^x A^x - u^y A^y - u^z A^z =$$
$$= A^t + \sigma\dot\theta sin(\theta) \left(cos(\theta) A^r - sin(\theta) A^\theta \right) - \sigma\dot\theta cos(\theta) \left(sin(\theta) A^r + cos(\theta) A^\theta \right) =$$
$$= A^t - \sigma\dot\theta A^\theta$$

Putting everything into the action, it becomes:

$$S = -T \int\!\!\!\int_{(0,-l_2)}^{(T,l_1)} \mathrm{d}\sigma\mathrm{d}t \sqrt{1 + \sigma^2 \left(\theta'^2 - \dot\theta^2 \right)} - m \int_0^T \mathrm{d}t \sqrt{1 - \sigma^2\dot\theta^2}|_{\sigma=-l_2}^{\sigma=l_1} - q \int_0^T \left(A^t - \sigma\dot\theta A^\theta \right) \mathrm{d}t|_{\sigma=-l_2}^{\sigma=l_1}$$

(69)

21

2.2 The Spinning String Ansatz

Throughout our analysis we will assume the string to be rotating with a constant angular velocity. In the static gauge 68 this amounts to setting $\dot{\theta} = \omega$. More explicitly we have

$$x = (\tau, \sigma \cos(\omega\tau), \sigma \sin(\omega\tau)) \tag{70a}$$

And for the second end point

$$x_{opposite} = (\tau, \sigma \cos(\omega\tau + \pi), \sigma \sin(\omega\tau + \pi)) \tag{70b}$$

2.3 The Electromagnetic Fields

The Lienard-Wichert formulas for the fields of a point charge are [22]:

$$\theta(\vec{x}, t) = \left[\frac{e}{\left(1 - \vec{\beta} \cdot \vec{n}\right) R} \right]_{ret} \tag{71a}$$

$$\vec{A}(\vec{x}, t) = \left[\frac{e\vec{\beta}}{\left(1 - \vec{\beta} \cdot \vec{n}\right) R} \right]_{ret} \tag{71b}$$

$$\vec{E}(\vec{x}, t) = \left[e \frac{\vec{n} - \vec{\beta}}{\gamma^2 \left(1 - \vec{\beta} \cdot \vec{n}\right)^3 R^2} + \frac{e}{c} \frac{\vec{n} \times \left\{ \left(\vec{n} - \vec{\beta}\right) \times \dot{\vec{\beta}} \right\}}{\left(1 - \vec{\beta} \cdot \vec{n}\right)^3 R} \right]_{ret} \tag{71c}$$

$$\vec{B}(\vec{x}, t) = \left[\vec{n} \times \vec{E} \right]_{ret} \tag{71d}$$

Where

- $\vec{\beta}$ is the velocity of the point charge source, divided by c.

- $\gamma = \left(1 - \beta^2\right)^{-1/2}$

- $\vec{n}$ is the unit vector from the source to the point where we evaluate the fields.

- R is the distance from the source to the point where we evaluate the fields.

- e is the charge of the source.

- R_{ret} denotes the distance from the source at retarded time to the point where we evaluate the fields.

- The formulas are evaluated with the retardation condition (also called the light cone condition) $t - t_{ret} = R_{ret}$
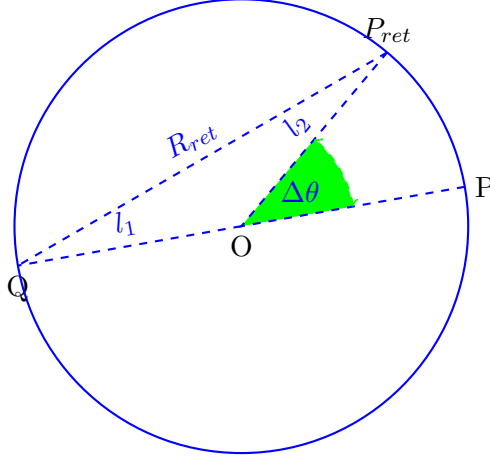
Figure 4: The geometry of the system. The points Q, P and P_{ret} are the "receiving" particle, the emitting particle and the position of the emitting particle at retarded time, respectively. $\Delta\theta$ is the so called retardation angle. l_1 and l_2 are the respective radii of rotation and R_{ret} is the retarded distance.

We will see shortly that the key quantities will be the velocities of the quarks β_1, β_2 and the retardation angle $\Delta\theta$ defined in figure 4. Looking at figure 4 we can use the cosine law to relate the retardation angle with the retarded distance R_{ret}:

$$R_{ret}^2 = l_1^2 + l_2^2 - 2l_1 l_2 \cos(\pi - \Delta\theta)$$

By the definition of the retarded time, it is both ($c = 1$):

- The time it takes the light signal to get from P_{ret} to Q. $t - t_{ret} = R_{ret}$

- The time it takes the emitting particle to get from P_{ret} to P. $\omega l_2 (t - t_{ret}) = l_2 \Delta\theta$

Where ω is the rate of rotation of both particles. The conclusion being that $\frac{\Delta\theta}{\omega} = R_{ret}$. Combining this with the cosine law result gives:

$$\Delta\theta^2 = \beta_1^2 + \beta_2^2 + 2\beta_1\beta_2 cos(\Delta\theta) \tag{72}$$

Here $\beta_i = \omega l_i$. This condition relates the retardation angle $\Delta\theta$ and the velocities of the string end points. This equation is solved numerically, giving implicitly the function $\Delta\theta = f(\beta_1)$. It can also be solved approximately by guessing a power series solution (in powers of β or $1 - \beta$) and solving for the coefficients iteratively.

The calculation of the various fields is then reduced to a geometric calculation where everything will depend on the length of the string and the rate of rotation.

23

The result for the electromagnetic fields and potentials:

$$A^0\left(l_1\right) = \frac{q_2\omega}{\beta_1\beta_2\sin(\Delta\theta)+\Delta\theta} \tag{73a}$$

$$A^\theta\left(l_1\right) = -\frac{\beta_2 q_2\omega\cos(\Delta\theta)}{\beta_1\beta_2\sin(\Delta\theta)+\Delta\theta} \tag{73b}$$

$$\vec{E} = \left\{ \begin{array}{c} \frac{q_2\omega^2\left(2\beta_2\left(\beta_1^2-\Delta\theta^2+1\right)\cos(\Delta\theta)+\beta_1\beta_2^2\cos(2\Delta\theta)+\beta_1\beta_2^2+2\beta_1+2\beta_2\Delta\theta\sin(\Delta\theta)\right)}{2(\beta_1\beta_2\sin(\Delta\theta)+\Delta\theta)^3} \\ -\frac{\beta_2 q_2\omega^2\left(\beta_1\beta_2(\sin(2\Delta\theta)-2\Delta\theta)-2\left(\Delta\theta^2-1\right)\sin(\Delta\theta)-2\Delta\theta\cos(\Delta\theta)\right)}{2(\beta_1\beta_2\sin(\Delta\theta)+\Delta\theta)^3} \\ 0 \end{array} \right\} \tag{73c}$$

$$\vec{B} = \left\{ \begin{array}{c} 0 \\ 0 \\ \frac{\beta_2 q_2\omega^2\left(\beta_1^2\beta_2+\beta_1\left(\beta_2^2+1\right)\cos(\Delta\theta)+\beta_1\Delta\theta\sin(\Delta\theta)+\beta_2\right)}{(\beta_1\beta_2\sin(\Delta\theta)+\Delta\theta)^3} \end{array} \right\} \tag{73d}$$

Which was obtained using Mathematica. To see that this complicated expression makes physical sense we calculate it in the non-relativistic limit. In this limit we have

$$\beta \to 0 \tag{74a}$$

$$\beta_1 \to \beta \qquad\qquad \beta_2 \to \beta \tag{74b}$$

$$\Delta\theta \to 2\beta \qquad\qquad \omega \to \frac{2\beta}{L} \tag{74c}$$

$$\tag{74d}$$

Using these we calculate the limits for the fields and potentials and get:

$$A^0\left(l_1\right) = \frac{q_2}{L} \tag{75a}$$

$$A^\theta\left(l_1\right) = -\frac{\beta q_2}{L} \tag{75b}$$

$$\vec{E} = \left\{ \begin{array}{c} \frac{q_2}{L^2} \\ 0 \\ 0 \end{array} \right\} \qquad\qquad \vec{B} = \left\{ \begin{array}{c} 0 \\ 0 \\ \frac{\beta q_2}{L^2} \end{array} \right\} \tag{75c}$$

This shows that when $\beta = 0$ we have no magnetic field and only an electrostatic field. The fields when the velocities (and masses) are identical are:

$$\vec{E} = \left\{ \begin{array}{c} \frac{\beta q_2 \omega^2 \left(2\left(\beta^2-\Delta\theta^2+1\right)\cos(\Delta\theta)+\beta^2\cos(2\Delta\theta)+\beta^2+2\Delta\theta\sin(\Delta\theta)+2\right)}{2(\beta^2\sin(\Delta\theta)+\Delta\theta)^3} \\ \frac{\beta q_2 \omega^2 \left(\sin(\Delta\theta)\left(\beta^2(-\cos(\Delta\theta))+\Delta\theta^2-1\right)+\beta^2\Delta\theta+\Delta\theta\cos(\Delta\theta)\right)}{(\beta^2\sin(\Delta\theta)+\Delta\theta)^3} \\ 0 \end{array} \right\} \quad (76a)$$

$$\vec{B} = \left\{ \begin{array}{c} 0 \\ 0 \\ \frac{\beta^2 q_2 \omega^2 \left(\left(\beta^2+1\right)\cos(\Delta\theta)+\beta^2+\Delta\theta\sin(\Delta\theta)+1\right)}{(\beta^2\sin(\Delta\theta)+\Delta\theta)^3} \end{array} \right\} \quad (76b)$$

We can use this form to take the relativistic limit $\beta = 1$.

$$\vec{E} = \left\{ \begin{array}{c} \frac{q_2\left(-2\left(\Delta\theta^2-2\right)\cos(\Delta\theta)+2\Delta\theta\sin(\Delta\theta)+\cos(2\Delta\theta)+3\right)}{2l^2(\Delta\theta+\sin(\Delta\theta))^3} \\ \frac{q_2\left(\left(\Delta\theta^2-1\right)\sin(\Delta\theta)+\Delta\theta+(\Delta\theta-\sin(\Delta\theta))\cos(\Delta\theta)\right)}{l^2(\Delta\theta+\sin(\Delta\theta))^3} \\ 0 \end{array} \right\} \quad (77a)$$

$$\vec{B} = \left\{ \begin{array}{c} 0 \\ 0 \\ \frac{q_2(\Delta\theta\sin(\Delta\theta)+2\cos(\Delta\theta)+2)}{l^2(\Delta\theta+\sin(\Delta\theta))^3} \end{array} \right\} \quad (77b)$$

We can also solve for $\Delta\theta$ in that limit and get $\Delta\theta = 1.47817 \approx 0.47\pi$. Setting into the above fields yields:

$$\vec{E} = \left\{ \begin{array}{c} \frac{0.162696 q_2}{l^2} \\ \frac{0.178509 q_2}{l^2} \\ 0 \end{array} \right\} \quad (78a)$$

$$\vec{B} = \left\{ \begin{array}{c} 0 \\ 0 \\ \frac{0.241527 q_2}{l^2} \end{array} \right\} \quad (78b)$$

Calculating the norm of the electric fields gives $|\vec{E}| = \frac{0.241527 q_2}{l^2}$ which is exactly the norm of the magnetic field (given by it's third component). We will use equations 73 in the next sections.

2.4 The Equations of Motion

2.4.1 Combining Fields and Point Particles

In combining point particle lagrangians and field lagrangian densities, we obtain slightly non standard Euler Lagrange equations. The action is the sum: $S = \int \mathcal{L} d^2\sigma + \int L d\tau$ where $\mathcal{L}$ is a lagrangian density and L is a

lagrangian. We obtain the equations of motion by varying the solution by an infinitesimal function $\delta x^\mu(\sigma, \tau)$ such that $\delta x^\mu(0) = \delta x^\mu(T) = 0$

$$\delta S = \int \left(\frac{\partial \mathcal{L}}{\partial x^\mu} \delta x^\mu + \frac{\partial \mathcal{L}}{\partial(\partial_\alpha x^\mu)} \partial_\alpha \delta x^\mu \right) d^2\sigma + \sum_{\sigma=l_1,-l_2} \int \left(\frac{\partial L}{\partial x^\mu} \delta x^\mu + \frac{\partial L}{\partial(\partial_\tau x^\mu)} \partial_\tau \delta x^\mu \right) d\tau$$

Integrating this by parts we get

$$\delta S = \int \left(\frac{\partial \mathcal{L}}{\partial x^\mu} - \partial_\alpha \left(\frac{\partial \mathcal{L}}{\partial(\partial_\alpha x^\mu)} \right) \right) \delta x^\mu d^2\sigma + \int \left(\frac{\partial L}{\partial x^\mu} - \partial_\tau \left(\frac{\partial L}{\partial(\partial_\tau x^\mu)} \right) + \frac{\partial \mathcal{L}}{\partial(\partial_\sigma x^\mu)} \right) |^{\sigma=l_1} \delta x^\mu d\tau +$$

$$\int \left(\frac{\partial L}{\partial x^\mu} - \partial_\tau \left(\frac{\partial L}{\partial(\partial_\tau x^\mu)} \right) - \frac{\partial \mathcal{L}}{\partial(\partial_\sigma x^\mu)} \right) |^{\sigma=-l_2} \delta x^\mu d\tau$$

So requiring no variation to first order in the action gives us the Euler Lagrange equations of motion for the field:

$$\frac{\partial \mathcal{L}}{\partial x^\mu} - \partial_\alpha \left(\frac{\partial \mathcal{L}}{\partial(\partial_\alpha x^\mu)} \right) = 0 \tag{79}$$

and for the end points:

$$\frac{\partial L}{\partial x^\mu}_{\sigma=l_1} - \partial_\tau \left(\frac{\partial L}{\partial(\partial_\tau x^\mu)} \right)_{\sigma=l_1} + \frac{\partial \mathcal{L}}{\partial(\partial_\sigma x^\mu)}_{\sigma=l_1} = 0 \tag{80a}$$

$$\frac{\partial L}{\partial x^\mu}_{\sigma=-l_2} - \partial_\tau \left(\frac{\partial L}{\partial(\partial_\tau x^\mu)} \right)_{\sigma=-l_2} - \frac{\partial \mathcal{L}}{\partial(\partial_\sigma x^\mu)}_{\sigma=-l_2} = 0 \tag{80b}$$

For stationary end points we could have taken $\delta x^\mu_{\sigma=l_1,-l_2} = 0$ for $\mu \neq 0$ (Dirichlet boundary conditions). We will use the first boundary condition eq 80, as the string endpoints are free to move.

2.4.2 The Boundary Equations

We turn to the boundary equations and write it explicitly and get boundary equations for the end points. We first express the following derivatives:

$$\frac{\partial L}{\partial x^\mu} = -q_1 u^\nu \frac{\partial A_\nu(l_1)}{\partial x^\mu} - q_2 u^\nu \frac{\partial A_\nu(l_2)}{\partial x^\mu} \tag{81}$$

$$\partial_\tau \frac{\partial L}{\partial(\partial_\tau x^\mu)} = -m_1 \partial_\tau \left(\frac{u_\mu}{\sqrt{u^\nu u_\nu}} \right) - m_2 \partial_\tau \left(\frac{u_\mu}{\sqrt{u^\nu u_\nu}} \right) - q_1 u^\nu \frac{\partial A_\mu(l_1)}{\partial x^\nu} - q_2 u^\nu \frac{\partial A_\mu(l_2)}{\partial x^\nu} \tag{82}$$

$$\frac{\partial \mathcal{L}}{\partial(\partial_\sigma x^\mu)} = -T \frac{(u \cdot V) u_\mu - u^2 V_\mu}{\sqrt{(u \cdot V)^2 - u^2 V^2}} \tag{83}$$

Equation 80 for $\sigma = l_1$ is then

$$m_1 \partial_\tau \left(\frac{u_\mu}{\sqrt{u^\nu u_\nu}} \right) - q_1 u^\nu \frac{\partial A_\nu (l_1)}{\partial x^\mu} + q_1 u^\nu \frac{\partial A_\mu (l_1)}{\partial x^\nu} - T \frac{(u \cdot V) u_\mu - u^2 V_\mu}{\sqrt{(u \cdot V)^2 - u^2 V^2}} = 0$$

Which can be written in terms of the electromagnetic fields as:

$$m_1 \partial_\tau \left(\frac{u_\mu}{\sqrt{u^\nu u_\nu}} \right) + q_1 u^\nu F_{\nu\mu} (l_1) - T \frac{(u \cdot V) u_\mu - u^2 V_\mu}{\sqrt{(u \cdot V)^2 - u^2 V^2}} \Big|_{\sigma = l_1} = 0$$

Inserting the spinning string solution 70, we specialize to one axis $\mu = 1$ and get:

$$m_1 \frac{\omega^2 l_1 cos(\omega\tau)}{\sqrt{1 - \omega^2 l_1^2}} + q_1 \omega l_1 cos(\omega\tau) B_3 (l_1) + q_1 E_1 (l_1) - T\sqrt{1 - \omega^2 l_1^2} cos(\omega\tau) = 0$$

$$(84)$$

We want the equation in the radial direction, so we also specialize to $\tau = 0$, and in terms of $\beta_i = \omega l_i$ and $\gamma_i = \left(1 - \beta_i^2 \right)^{-1/2}$ this is:

$$m_1 \frac{\omega\beta_1}{\sqrt{1 - \beta_1^2}} + q_1 \beta_1 B_3 (l_1) + q_1 E_1 (l_1) - T\sqrt{1 - \beta_1^2} = 0 \qquad (85)$$

We can see a string tension term, a centrifugal term and an electromagnetic term. This equation constitutes a constraint implicitly giving $\omega = \omega (\beta_1, \beta_2, m_1, m_2, q_1, q_2, T)$. Using the fact that $T, q_1 q_2, \omega$ and $\Delta\theta$ are the same for both end points, the force equations for the two end points also provide a relation between $\{m_1, m_2, \beta_1, \beta_2\}$. In the case of $q_1 q_2 = 0$ it is just:

$$\gamma_1^2 \beta_1 m_1 \omega = T = \gamma_2^2 \beta_2 m_2 \omega \qquad (86)$$

In the case of equal end point masses the velocities must be equal. This extends into the case of $q_1 q_2 \neq 0$ where the endpoint velocities must still be equal from symmetry. Plugging in the electromagnetic fields (equation 73) into the equation for one of the particles we get:

$$\frac{\pi\omega^2(a - S)}{2(\beta_1 + \beta_2)^2} - \frac{\beta_1 m_1 \omega}{\sqrt{1 - \beta_1^2}} + T\sqrt{1 - \beta_1^2} + \qquad (87)$$

$$- q_1 q_2 \omega^2 \frac{\beta_1 \left(2\beta_1^2 \beta_2^2 + 2\beta_1 \left(\beta_2^2 + 1 \right) \beta_2 \cos(\Delta\theta) + 2\beta_1 \beta_2 \Delta\theta \sin(\Delta\theta) + 3\beta_2^2 + 2 \right)}{2(\beta_1 \beta_2 \sin(\Delta\theta) + \Delta\theta)^3} +$$

$$- q_1 q_2 \omega^2 \frac{\beta_2 \left(\left(\beta_1^2 - 2\Delta\theta^2 + 2 \right) \cos(\Delta\theta) + \beta_1^2 \cos(\Delta\theta) + \beta_1 \beta_2 \cos(2\Delta\theta) + 2\Delta\theta \sin(\Delta\theta) \right)}{2(\beta_1 \beta_2 \sin(\Delta\theta) + \Delta\theta)^3} = 0$$

A note on this equation is that here we only deal with it's radial component. The reason is that the angular component cannot be satisfied: it only contains electromagnetic contributions which do not cancel. The underlying issue is that we neglect the radiation emitted by the system, which is a good approximation when it would take many times the particles' lifetime to radiate a large proportion of the system's energy. This calculation is carried out in detail in appendix B.

The next issue is the manner of solving these equations. Trying to solve the equations as they are is a very involved and computationally intensive issue. A first approximation we can make to simplify this issue is to solve for one of the particles and take the velocity relation to be equation 86. The approximation we are making is assuming the electromagnetic forces are small enough relative to the other forces so that the velocity relation doesn't change. When the velocities are equal the electromagnetic contribution to the velocity relation (86) vanishes, so that this approximation is exact when taking the masses equal. This approximation can be checked by solving the equations of motion (within the approximation) and checking the magnitude of the electromagnetic force relative to the others at the solution. This is calculated and presented in figure 5 .Note that the electromagnetic force is always small relative to at least two forces. In figure 6 the electromagnetic contribution to the velocity relation is calculated (having took 86 as the velocity relation) in units of $m_1\gamma_1^2\beta_1$. The error is dependent both on the velocity and on the mass ratio. This shows that our procedure is not entirely consistent. Nevertheless this does not effect the ability of the model to fit to experimental Regge trajectories. Light flavourless hadrons involve up and down quarks which have essentially the same mass, so these fit well with the approximation. On the other hand we have hadrons involving charm quarks which are very massive, but typically the velocities involved are very large, so again the error is small. There could still be a problem with strange hadrons such as the Kaon. In particular, the fits we calculated were taken to have a mass ratio of identity, where the approximation is exact. We will encounter some difficulties in the mass difference section, and these might be explained as consequences of our approximation and the symmetric assumption. We have attempted to solve the problem numerically with no approximation in the asymmetric case, but with no success so far.
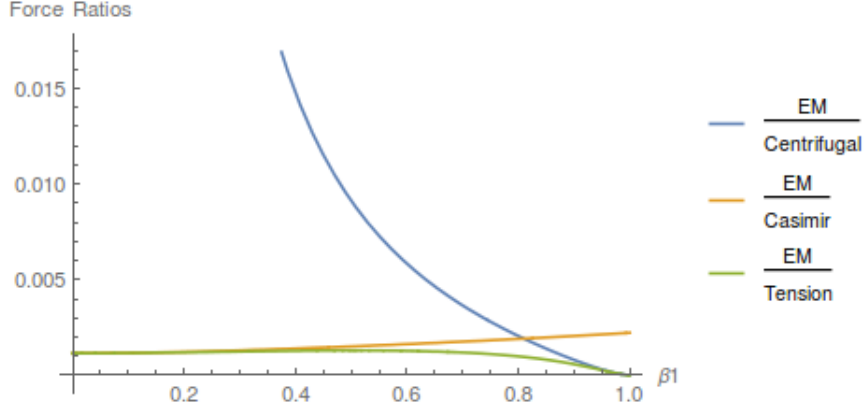
Figure 5: Ratios of electromagnetic force to other forces for realistic parameters. Note the casimir force is included, as explained later.
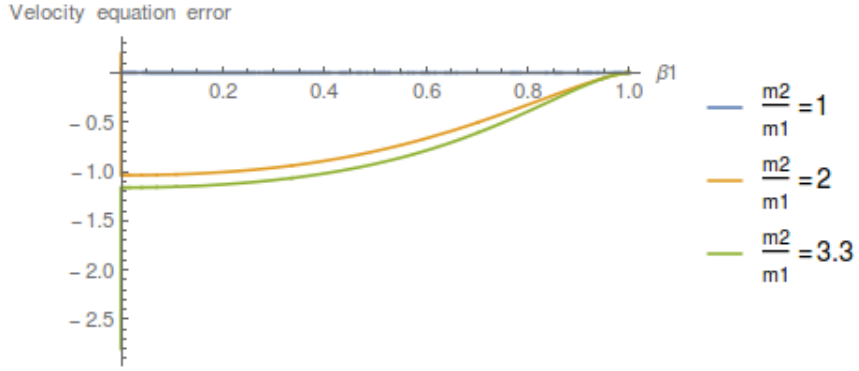

Figure 6: The neglected terms in the velocity relation in units of $m_1\gamma_1^2\beta_1$ for varying mass ratios.

2.4.3 The String Equations

We wish to verify that the spinning string ansatz 70 is truly a solution to the equations of motion.

Using the following derivatives:

$$\frac{\partial\mathcal{L}}{\partial(\partial_\tau x^\mu)} = \frac{\partial\mathcal{L}}{\partial u^\mu} = -T\frac{V_\mu\,(u\cdot V) - u_\mu V^2}{\sqrt{(u\cdot V)^2 - u^2 V^2}}$$

$$\frac{\partial\mathcal{L}}{\partial(\partial_\sigma x^\mu)} = \frac{\partial\mathcal{L}}{\partial V^\mu} = -T\frac{u_\mu\,(u\cdot V) - u^2 V_\mu}{\sqrt{(u\cdot V)^2 - u^2 V^2}}$$

The equation of motion 79 is then:

$$-\partial_\tau\left(-T\frac{V_\mu\left(u\cdot V\right)-u_\mu V^2}{\sqrt{\left(u\cdot V\right)^2-u^2V^2}}\right)-\partial_\sigma\left(-T\frac{u_\mu\left(u\cdot V\right)-u^2V_\mu}{\sqrt{\left(u\cdot V\right)^2-u^2V^2}}\right)=0$$

Putting in the spinning string solution 70 we get

$$\frac{-\partial_\tau u_\mu}{\sqrt{1-\omega^2\sigma^2}}+\frac{-\omega^2\sigma}{\sqrt{1-\omega^2\sigma^2}}V_\mu+\sqrt{1-\omega^2\sigma^2}\partial_\sigma V_\mu=0$$
$$-\partial_\tau u_\mu-\omega^2\sigma V_\mu+\left(1-\omega^2\sigma^2\right)\partial_\sigma V_\mu=0$$

The time-like equation is trivially satisfied ($V_0=\partial_\tau u_0=0$). In the spatial components, for example $\mu=1$, we get:

$$\omega^2\sigma cos\left(\omega\tau\right)+\omega^2\sigma cos\left(\omega\tau\right)-\left(1-\omega^2\sigma^2\right)\partial_\sigma cos\left(\omega\tau\right)=0$$

Which demonstrates the equations are satisfied.

2.5   The Energy

Calculating the energy can be done in two ways. Either as the generator of poincare time translations, or as the hamiltonian of the gauge fixed system. We show the second choice here:

$$E=\int d\sigma\left(\frac{\partial\mathcal{L}}{\partial\dot\theta}\dot\theta-\mathcal{L}\right)+\frac{\partial L}{\partial\dot\theta}\dot\theta-L$$
$$=T\int_{-l_2}^{l_1}d\sigma\frac{1+\sigma^2\theta'^2}{\sqrt{1+\sigma^2\left(\theta'^2-\dot\theta^2\right)}}+m\frac{1}{\sqrt{1-\sigma^2\dot\theta^2}}|_{\sigma=-l_2}^{\sigma=l_1}+q_1A^t\left(l_1\right)$$

Notice in the electromagnetic part we took just one contribution out of the two end points. This is because it already contains the coulomb interaction energy, and taking both contibutions would constitute taking it twice.

Inserting the spinning string solution 70 and electromagnetic potential 73 we get

$$E=T\int_{-l_2}^{l_1}d\sigma\frac{1}{\sqrt{1-\omega^2\sigma^2}}+m\frac{1}{\sqrt{1-\sigma^2\omega^2}}|_{-l_2}^{l_1}+\frac{q_1q_2\omega}{\beta_1\beta_2\sin(\Delta\theta)+\Delta\theta}=$$
$$=T\frac{sin^{-1}(\beta_1)}{\omega}+T\frac{sin^{-1}(\beta_2)}{\omega}+\frac{m_1}{\sqrt{1-\beta_1^2}}+\frac{m_2}{\sqrt{1-\beta_2^2}}+\frac{q_1q_2\omega}{\beta_1\beta_2\sin(\Delta\theta)+\Delta\theta}$$
$$\tag{88}$$

2.6 The Angular Momentum

The angular momentum is obtained as the generator of rotations. For the rotations in the rotation plane of the string:

$$J = \int d\sigma \frac{\partial \mathcal{L}}{\partial \dot\theta} + \frac{\partial L}{\partial \dot\theta} =$$

$$= T \int_{-l_2}^{l_1} d\sigma \frac{\sigma^2 \dot\theta}{\sqrt{1 + \sigma^2 \left(\theta'^2 - \dot\theta^2\right)}} + m_1 \frac{l_1^2 \dot\theta}{\sqrt{1 - l_1^2 \dot\theta^2}} + m_2 \frac{l_2^2 \dot\theta}{\sqrt{1 - l_2^2 \dot\theta^2}} + q_1 l_1 A^\theta(l_1) + q_2 l_2 A^\theta(l_2)$$

Inserting the spinning string solution 70 and electromagnetic potential 73 we get

$$J = T \int_{-l_2}^{l_1} d\sigma \frac{\sigma^2 \omega}{\sqrt{1 - \sigma^2 \omega^2}} + m_1 \frac{l_1^2 \omega}{\sqrt{1 - l_1^2 \omega^2}} + m_2 \frac{l_2^2 \omega}{\sqrt{1 - l_2^2 \omega^2}} +$$

$$- q_1 q_2 \frac{\beta_1 \beta_2 \cos(\Delta\theta)}{\beta_1 \beta_2 \sin(\Delta\theta) + \Delta\theta} - q_1 q_2 \frac{\beta_1 \beta_2 \cos(\Delta\theta)}{\beta_1 \beta_2 \sin(\Delta\theta) + \Delta\theta} =$$

$$= T \frac{-\frac{\beta_1}{\gamma_1} + sin^{-1}(\beta_1) - \frac{\beta_2}{\gamma_2} + sin^{-1}(\beta_2)}{2\omega^2} + m_1 \frac{\gamma_1 \beta_1^2}{\omega} + m_2 \frac{\gamma_2 \beta_2^2}{\omega} - q_1 q_2 \frac{2\beta_1 \beta_2 \cos(\Delta\theta)}{\beta_1 \beta_2 \sin(\Delta\theta) + \Delta\theta}$$

$$(89)$$

2.7 The Regge Trajectories and the Regge Intercept

Plotting $\left(J, E^2\right)$ as a function of β_1 gives the predicted classical Regge trajectories. In order to account for the observed intercept in the Regge trajectories we can add it in using three methods:

1. Put an intercept by hand into the angular momentum: $J \to J + a$

2. Put an intercept by hand into the energy squared: $\alpha' E^2 \to \alpha' E^2 - a$

3. Introduce a casimir energy $E_{casimir} = -\frac{\pi}{2} \frac{\tilde{a}}{L}$ which also induces a force and an intercept.

The first and second methods are the simplest phenomenological ways to introduce an intercept. The first has been used in [13] and [14]. The second method was used by us as a warm-up exercise and has given identical results. While these are good for an initial assessment of the model by comparing with regge trajectories, they suffer from a number of practical problems. First, there is no clear connection of the intercept and the dynamical mechanism which generated it. Second, the string tends to shrink to zero size, which can be problematic for some $J = 0$ states.

The following two subsections describe the analysis of the trajectories in the third method above.

2.7.1 The Casimir Energy Prescription

In the last option the induced force is

$$F_{casimir} = -\frac{d}{dL}E_{casimir} = -\frac{\pi}{2}\frac{\tilde{a}}{L^2} \tag{90}$$

This force is attractive for $\tilde{a} > 0$ and repulsive for $\tilde{a} < 0$. Notice this energy term has exactly the form of the quantum correction to the string potential (equation 57) induced by the quantum zero mode energy corrections. $\tilde{a}$ parametrizes the (quark mass dependent) sum over the zero mode frequencies, and turns out to be attractive for the case of zero masses ($\tilde{a} = \frac{(D-2)}{12} > 0$). If the casimir force is repulsive it can prevent the system from collapsing to zero size when there is no spin and the electromagnetic force is attractive (leaving no other force to balance the attraction). So we limit the parameter $\tilde{a} < 0$. The force is radial and so does not contribute to angular momentum.

Adding the appropriate terms to the expressions for the energy and boundary equations, the equations for construction of the regge trajectories are then:

$$E = \frac{T}{\omega}\left(\sin^{-1}(\beta_1) + \sin^{-1}(\beta_2)\right) + \gamma_1 m_1 + \gamma_2 m_2 + \frac{q_1 q_2 \omega}{\beta_1 \beta_2 \sin(\Delta\theta) + \Delta\theta} - \frac{\pi}{2}\frac{\tilde{a}\omega}{\beta_1 + \beta_2} \tag{91a}$$

$$J = T\frac{-\frac{\beta_1}{\gamma_1} + sin^{-1}(\beta_1) - \frac{\beta_2}{\gamma_2} + sin^{-1}(\beta_2)}{2\omega^2} + m_1\frac{\gamma_1\beta_1^2}{\omega} + m_2\frac{\gamma_2\beta_2^2}{\omega} - 2q_1 q_2 \beta_1 \beta_2 \frac{cos(\Delta\theta)}{\beta_1\beta_2 sin(\Delta\theta) + \Delta\theta} \tag{91b}$$

$$\Delta\theta^2 = \beta_1^2 + \beta_2^2 + 2\beta_1\beta_2 cos(\Delta\theta) \tag{91c}$$

$$\gamma_1^2 \beta_1 m_1 = \gamma_2^2 \beta_2 m_2 \tag{91d}$$

$$\frac{\pi\omega^2(a-S)}{2(\beta_1+\beta_2)^2} - \frac{\beta_1 m_1 \omega}{\sqrt{1-\beta_1^2}} + T\sqrt{1-\beta_1^2} + \tag{91e}$$

$$- q_1 q_2 \omega^2 \frac{\beta_1\left(2\beta_1^2\beta_2^2 + 2\beta_1\left(\beta_2^2+1\right)\beta_2\cos(\Delta\theta) + 2\beta_1\beta_2\Delta\theta\sin(\Delta\theta) + 3\beta_2^2 + 2\right)}{2(\beta_1\beta_2\sin(\Delta\theta) + \Delta\theta)^3} +$$

$$- q_1 q_2 \omega^2 \frac{\beta_2\left(\left(\beta_1^2 - 2\Delta\theta^2 + 2\right)\cos(\Delta\theta) + \beta_1^2\cos(\Delta\theta) + \beta_1\beta_2\cos(2\Delta\theta) + 2\Delta\theta\sin(\Delta\theta)\right)}{2(\beta_1\beta_2\sin(\Delta\theta) + \Delta\theta)^3} = 0$$

We can obtain analytic expressions for the regge trajectory in the two following limits:

- $\beta \to 0$: In this limit the quarks are slowly moving, implying most of the energy is related to the string and end points and the quarks are heavy.

- $\beta \to 1$: In this limit the quarks are relativistic, implying most of the energy is related to the motion and the quarks are light.

In both cases we expand the energy and angular momentum around the limit, obtaining series of either β or $(1 - \beta)$. From the series for the energy $E = f(\beta)$ (or $E = f(1 - \beta)$) we calculate the inverse series $\beta = f^{-1}(E)$ or $1 - \beta = f^{-1}(E)$. This can then be inserted into the power series for the angular momentum, and obtain the regge trajectory $J(E)$. This process is automated using computer algebra systems (Mathematica in our case). The code is shown in section D.

In section 3.1 we present the numerical fits to PDG data, and determine values for the slope and endpoint masses. It is also beneficial to obtain analytic expressions for the Regge trajectories, which we can compare with the corresponding expressions for the uncharged model, as well as see what is the effect of the charge on the trajectory.

2.7.2 The Light Quark Limit

We proceed to derive analytic expressions for the Regge trajectory in the light quark limit. In this limit the quark velocity is large, $\beta = 1 - \epsilon^2$, $\epsilon \to 0$. The result when adding massive end points is:

$$J = \alpha' E^2 \left(1 - \frac{4\sqrt{\pi}}{3} \left(\frac{1}{E} \right)^{3/2} \left(m_1^{3/2} + m_2^{3/2} \right) + \frac{1}{5} \pi^{3/2} \left(\frac{1}{E} \right)^{5/2} \left(m_1^{5/2} + m_2^{5/2} \right) \right)$$
$$+ O \left(\frac{1}{E} \right)^3 \tag{92a}$$

The result when adding casimir forces and charges as well is:

$$J = \frac{1}{4} \pi \tilde{a} - 0.479 q_1 q_2 + \alpha' E^2 - \frac{1}{3} 4\sqrt{\pi} \left(m_1^{3/2} + m_2^{3/2} \right) \alpha' \sqrt{E} + \frac{\pi^{3/2} \alpha' \left(m_1^{5/2} + m_2^{5/2} \right)}{5 \sqrt{E}}$$
$$\tag{92b}$$

We see that $\tilde{a}$ is indeed an intercept in the relativistic limit, and that the electromagnetic interaction contributes an intercept as well.

2.7.3 The Heavy Quark Limit

We proceed to derive analytic expressions for the Regge trajectory in the heavy quark limit. In this limit the quark velocity is small, $\beta \to 0$. The equations are solved in the same manner. The result when adding massive

end points and no charge and casimir is:

$$
J = \frac{4}{3}\sqrt{\frac{2}{3}}\pi\alpha'\sqrt{\frac{m_1 m_2}{m_1 + m_2}}(E - m_1 - m_2)^{3/2} + \frac{7\sqrt{\frac{2}{3}}\pi\alpha'\left(m_1^2 - m_1 m_2 + m_2^2\right)(E - m_1 - m_2)^{5/2}}{27\sqrt{m_1 m_2(m_1 + m_2)^3}}
$$
$$
+ O\left((E - m_1 - m_2)^{7/2}\right) \tag{93a}
$$

The result for equal masses when adding casimir forces and charges is:

$$
J = \frac{\sqrt{\frac{\sqrt{T(-\pi\tilde{a} - 2q_1 q_2)}}{36m\sqrt{T(-\pi\tilde{a} - 2q_1 q_2)} + 3\sqrt{2}T(\pi\tilde{a} - 4q_1 q_2)}}\left(-6\sqrt{2}m\sqrt{T(-\pi\tilde{a} - 2q_1 q_2)} - \pi\tilde{a}T + 10q_1 q_2 T\right)}{2T} \times
$$
$$
\times \sqrt{E - 2m + \sqrt{2}\sqrt{T(-(\pi\tilde{a} + 2q_1 q_2))}} + O\left(E - 2m + \sqrt{2}\sqrt{T(-(\pi\tilde{a} + 2q_1 q_2))}\right)^{3/2} \tag{93b}
$$

2.8 The Mass Differences

[24] Due to confinement quarks are confined inside hadrons and are not observed as physical particles. Quark masses therefore cannot be measured directly and must be calculated indirectly through their influence on hadronic properties. Although we often speak of quark masses in the same terms as masses of the electron or muon, quantitative statements about the value of a quark mass must make careful reference to the particular theoretical model within which it is defined.

Historically, the first determinations of quark masses were performed using quark models. The resulting masses only make sense in the limited context of a particular quark model, and cannot be related to the quark mass parameters of the Standard Model. Non-relativistic quark models use constituent quark masses, which are of order 350 MeV for the u and d quarks. Constituent quark masses model the effects of dynamical chiral symmetry breaking which drives the hadronic masses Λ_{QCD}, and are not related to the quark mass parameters of the QCD Lagrangian. Constituent masses are only defined in the context of a particular hadronic model.

The QCD Lagrangian has a chiral symmetry in the limit that the quark masses vanish. This symmetry is spontaneously broken by dynamical chiral symmetry breaking, and explicitly broken by the quark masses. The non-perturbative scale of dynamical chiral symmetry breaking, Λ_χ, is around 1 GeV. It is conventional to call quarks heavy if $m > \Lambda_\chi$, so that explicit chiral symmetry breaking dominates (c,b, and t quarks are heavy), and light if $m < \Lambda_\chi$, so that spontaneous chiral symmetry breaking dominates (u,d and s quarks are light). At high energies or short distances, nonperturbative effects, such as chiral symmetry breaking, become small and one can, in principle, determine quark masses by analysing mass-dependent effects using QCD perturbation theory.

Similarly to the above situation, our model also determines quark masses by matching the model parameters with the desired results for observed hadronic properties. A particularly interesting property is the mass difference between hadrons of differing electromagnetic charge but identical Isospin, Baryon number, angular momentum and parity. It turns out that the difference in the mass of the quarks (which we would call in this case "current quarks" by analogy) can be determined without knowledge of the individual quark masses. This is similar in spirit to Isospin symmetry breaking where the degeneracy in the proton and neutron masses is broken by the difference in the masses of the u and d quarks.

Electromagnetic mass differences for hadrons are known for states with $J_{orbital} = 0$, therefore we first analyse the case of $\beta = 0$. Taking the limit $\beta \to 0$ we get the following energy, angular momentum and force equations (where L is the string length):

$$E = TL + m_1 + m_2 + \frac{q_1 q_2 - \frac{\pi}{2}\tilde{a}}{L} \tag{94a}$$

$$J = 0 \tag{94b}$$

$$\frac{q_1 q_2 - \frac{\pi}{2}\tilde{a}}{L^2} = T \tag{94c}$$

See appendix C for details of the derivation. Putting the two together we get

$$E = 2\sqrt{T}\sqrt{\frac{q_1 q_2}{137} - \frac{\pi}{2}\tilde{a}} + m_1 + m_2 \tag{95}$$

$$J = 0 \tag{96}$$

Where the parameters $\tilde{a}, T$ are measured from the Regge trajectory fits

When the charge is negligible relative to the casimir contribution we can approximate:

$$E \approx \frac{1}{\sqrt{\alpha'}}\sqrt{-\tilde{a}} + \frac{1}{\pi\sqrt{\alpha'}}\frac{\frac{q_1 q_2}{137}}{\sqrt{-\tilde{a}}} + m_1 + m_2$$

Taking the difference between masses of hadrons which correspond to differently charged versions of the same particle, for which the parameters a, S, α' are constants:

$$\Delta E \approx \frac{1}{137\pi\sqrt{\alpha'}}\frac{\Delta(q_1 q_2)}{\sqrt{-\tilde{a}}} + \Delta m_{quarks}$$

From the mass difference of the hadrons we can infer mass differences between the up and down quarks. For example the proton and neutron are considered as a quark-diquark system of $(ud - u)$ and $(ud - d)$ respectively, and so the end point masses are $m_u + m_d$ and $2m_d$ respectively. Furthermore

q_1q_2 is calculated as $q_{diquark}q_{quark}$ so that $q^2_{proton} = \left(\frac{2}{3} - \frac{1}{3}\right)\frac{2}{3} = \frac{2}{9}, q^2_{neutron} = -\left(\frac{2}{3} - \frac{1}{3}\right)\frac{1}{3} = -\frac{1}{9}$. If the hadron is a superposition of electromagnetic states (i.e. $\frac{1}{\sqrt{2}}\left(|u\bar{u}\rangle \pm |d\bar{d}\rangle\right)$) then q^2 is calculated as the average q^2.

$$M_{neutron} - M_{proton} = 2m_d - m_d - m_u + \frac{1}{137\pi\sqrt{\alpha'}}\frac{\left(-\frac{3}{9}\right)}{\sqrt{-\tilde{a}}} =$$
$$= m_d - m_u + \frac{1}{137\pi\sqrt{\alpha'}}\frac{\left(-\frac{3}{9}\right)}{\sqrt{-\tilde{a}}}$$

Reversing the argument, the difference in the up and down quark masses can be calculated from the hadron mass differences and the fit to the regge trajectory:

$$m_d - m_u = M_{neutron} - M_{proton} + \frac{1}{137\pi\sqrt{\alpha'}}\frac{\left(\frac{3}{9}\right)}{\sqrt{-\tilde{a}}}$$

Notice that this calculation does not involve the masses of the u and d quarks, so knowing them explicitly is not required. The slope and casimir term a are put in from the regge fits, so there is some implicit dependence on the endpoint masses. Also when dealing with baryons there is an ambiguity as of what quark and diquark to consider as lying at the ends of the string. The diquark charge is the sum of the charges of the quarks it is composed of, and the ambiguity consists of which quarks are chosen to form the diquark. In the calculations on section 2.8 we have eliminated this ambiguity by choosing that whenever possible, a diquark would be composed of oppositely charged quarks. This has the physical motivation that oppositely charged quarks should tend to form diquarks more that same charged ones.

The up and down quark mass differences depend crucially on the casimir coefficient and the hadron masses. When extracting the coefficient from the regge trajectories there is an implicit connection between the endpoint masses and the extracted casimir coefficient, but due to the large uncertainty in the endpoint masses there is also a large uncertainty in the casimir coefficient. On the other hand we can record the range of permitted coefficients and masses at some slope α' and input those into the calculation of the mass differences to get a corresponding range of mass differences for each hadron. Comparing the mass differences of u/d quarks between different hadrons should give consistent results (because the location of a flavour brane cannot depend on what kind of hadron one considers). The hope is that the range of consistent quark mass differences would be small, enabling a precise determination of the corresponding quark masses and casimir coefficients. Therefore it is expected that a consistent calculation of mass differences would place more strict bounds on the endpoint masses and the casimir coefficient.

Once the up and down quark mass differences are determined we can make predictions for hadronic electromagnetic mass differences for the states

with $J_{orbital} \neq 0$ using equations 98.This assumes the intercept does not depend on the rate of rotation. The calculation can be done numerically. Note that in this case the hadronic mass differences will generically depend on the absolute masses of the quarks instead of just their mass differences.

In section 3.2 we present the results of the calculation of the up/down mass difference for several different hadrons using the parameters consistent with the regge fits, and analyse the results.

3   Confronting with PDG Data

3.1   The Regge Trajectories

Using the methods outlined in the previous section, we numerically fit the Regge trajectories of our model to PDG data for the hadrons. We separate the treatment into the cases where the quark masses are approximately equal and the cases where the quark masses are expected to differ significantly. In the so called "symmetric" cases we assume $m_1 = m_2$ greatly simplifying the equations. This method is used to fit the trajectories of the flavourless hadrons, determining the approximately degenerate masses of the up and down quarks. In the case of greatly differing masses we take the first approximation that the larger mass is stationary, with the other mass orbiting it. This approximation is used in the cases of hadrons composed of one light quark and a heavy quark such as the D meson. The mass of the light quark is determined from the flavourless hadron fits, and we determine the mass of the charm quark. The case of the a light quark and a strange quark seems to be somewhat intermediate and we use the symmetric approximation in that case. It should be kept in mind the masses discussed here are neither constituent quark masses nor quark current masses, but are a new class of masses associated with the string hanging from the flavour brane. In both cases we take the electromagnetic fine structure constant $\alpha_e = \frac{1}{137}$.

In the case of equal quark masses the boundary equations, energy and angular momentum read:

$$E = \frac{2T}{\omega}\sin^{-1}(\beta)) + \gamma(m_1 + m_2) + \frac{q_1 q_2 \omega}{\beta^2 \sin(\Delta\theta) + \Delta\theta} - \frac{\pi}{4}\frac{\tilde{a}\omega}{\beta} \tag{97a}$$

$$J = T\frac{-\frac{\beta}{\gamma} + sin^{-1}(\beta)}{\omega^2} + (m_1 + m_2)\frac{\gamma\beta^2}{\omega} - 2q_1 q_2 \beta^2 \frac{cos(\Delta\theta)}{\beta^2 sin(\Delta\theta) + \Delta\theta} \tag{97b}$$

$$\Delta\theta^2 = 2\beta^2 + 2\beta^2 cos(\Delta\theta) \tag{97c}$$

$$\frac{\pi\omega^2(a-S)}{8\beta^2} - \frac{\beta m_1 \omega}{\sqrt{1-\beta^2}} + T\sqrt{1-\beta^2}+ \tag{97d}$$

$$- q_1 q_2 \omega^2 \frac{\beta\left(2\beta^4 + 2\beta^2\left(\beta^2 + 1\right)\cos(\Delta\theta) + 2\beta^2\Delta\theta\sin(\Delta\theta) + 3\beta^2 + 2\right)}{2(\beta^2\sin(\Delta\theta) + \Delta\theta)^3}+$$

$$- q_1 q_2 \omega^2 \frac{\beta\left(\left(\beta^2 - 2\Delta\theta^2 + 2\right)\cos(\Delta\theta) + \beta^2\cos(\Delta\theta) + \beta^2\cos(2\Delta\theta) + 2\Delta\theta\sin(\Delta\theta)\right)}{2(\beta^2\sin(\Delta\theta) + \Delta\theta)^3} = 0$$

In the case of one mass negligible with respect to the other the boundary equations, energy and angular momentum read:

$$E = \frac{TL}{\beta}\sin^{-1}(\beta) + \gamma m_1 + m_2 + \frac{q_1 q_2}{L} - \frac{\pi}{2}\frac{\tilde{a}}{L} \tag{98a}$$

$$J = TL^2\frac{-\frac{\beta}{\gamma} + sin^{-1}(\beta)}{2\beta^2} + m_1\gamma\beta L \tag{98b}$$

$$\frac{\pi(a-S)}{2L^2} - \frac{\gamma\beta^2 m_1}{L} + \frac{T}{\gamma} - \frac{q_1 q_2}{L^2} = 0 \tag{98c}$$

$$\Delta\theta = \beta \tag{98d}$$

Where we have set $\beta_2 = 0$ so that one of the endpoints is stationary, and L is the string length. Upon doing fits we see that typically the velocity of the light endpoint is such that γ is order one. The accuracy of the procedure can be estimated by observing that by the relation

$$\gamma_1^2 m_1 \beta_1 = \gamma_2^2 m_2 \beta_2$$

the velocity in next order of the "stationary" endpoint is

$$\beta_2^{(1)} \approx \frac{m_1}{m_2}\beta_1 \tag{99}$$

The leading correction to the energy comes from the stringy term and is approximately:

$$\Delta E \approx TL\frac{m_1}{m_2} \approx (E - m_1 - m_2)\frac{m_1}{m_2}$$

In the asymmetric fits we did to the D meson the correction to the energy is then 6% at the most, so the correction to E^2 and the trajectory would be less than 1%.

In previous work [13, 14] the model with no electric charge was confronted with PDG data. There the intercept was introduced by adding a constant to the angular momentum (method 1 discussed in section 2.7). When done in such a way, there is no way of distinguishing between fits to the total angular momentum J of a hadron, and fits to the orbital angular momentum $J_{orbital}$, of the same hadron, as the intercept could always be adjusted to give either plot. However when introducing an intercept using the casimir energy prescription we can clearly distinguish between the two fits. We find that we cannot fit the model to the total angular momentum J of the hadron. Examples for the ρ and K^* mesons can be seen in figure 7. The reason is that the casimir coefficient must be *repulsive* in order for the hadron to be stable at the limit where it is not spinning. As was mentioned in section 2.7 this is satisfied when $\tilde{a} < 0$. Under this limitation we cannot bring the trajectory to fit in the J plane. However when we plot the same trajectory in the (L, M^2) plane this intercept disappears: it is just the difference between J and L. Therefore, all the fits will be done for (L, E^2). In order to determine the orbital angular momentum from the total angular momentum and parity we use the relations:

$$J = L \pm S$$
$$P_{meson} = (-1)^{L+1}$$
$$P_{baryon} = (-1)^{L}$$
$$J = L \pm S$$

Where L, J is the orbital and total angular momentum respectively, P is the parity and S the hadronic intrinsic spin. In the context of the linear trajectories we have the relation

$$L = J - S = \alpha' E^2 + a - S \tag{100}$$

Where we can now identify

$$\tilde{a} = a - S \tag{101}$$

as the casimir coefficient when fitting to the orbital angular momentum.

In the following, we will present the goodness of the fit in the parameter space (m, α'), and determine values for the universal string tension and end point masses for various hadrons. The fits were done numerically in Mathematica 10. The goodness of fit is measured in terms of the dimensionless quantity:

$$\chi^2 = \frac{1}{N} \sum_{i \in trajectory} \left(\frac{M_{i,pdg}^2 - M_{i,model}^2}{M_{i,pdg}^2} \right)^2 \tag{102}$$
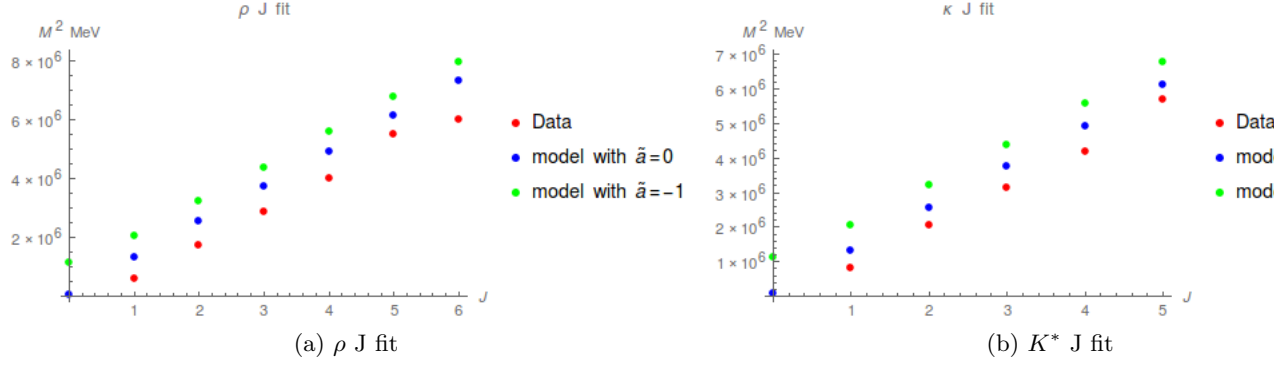
(a) ρ J fit

(b) K^* J fit

Figure 7: Fits to $\left(J, E^2\right)$ for the ρ and K^*.

| Quark type	Mass range $[MeV]$
u	150
d	152.1
s	345
c	1594

Table 2: Estimated quark masses. u/d mass difference is taken from mass difference calculation.

$M^2_{i,model}, M^2_{i,pdg}$ are the measured and calculated masses squared of the i-th particle in the trajectory. This quantity is calculated for any given fit. It is then used to compare different fits, with the linear fit as a reference. Figures 8,9,11 show the mass symmetric fits (endpoint masses assumed to be equal for simplicity),plotting $\frac{\chi^2}{\chi^2_{linear}}$ as a function of the endpoint masses m[MeV] (x-axis) and slope $\alpha'[MeV^{-2}]$ (y-axis). Tables 3,5 are summary tables showing the slope and endpoint masses obtained in the optimal symmetric fit. Tables 4,6 are the corresponding quantities obtained in references [13] and [14].

We can see that for the most part, the masses obtained in the two kinds of fits are comparable, while the slopes obtained are mostly inconsistent. From our Regge fit we can estimate the masses of the various quarks (see table 2).

(a) Pion fit

(b) ρ fit
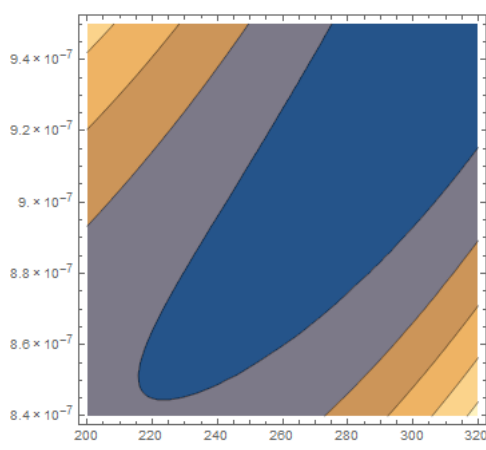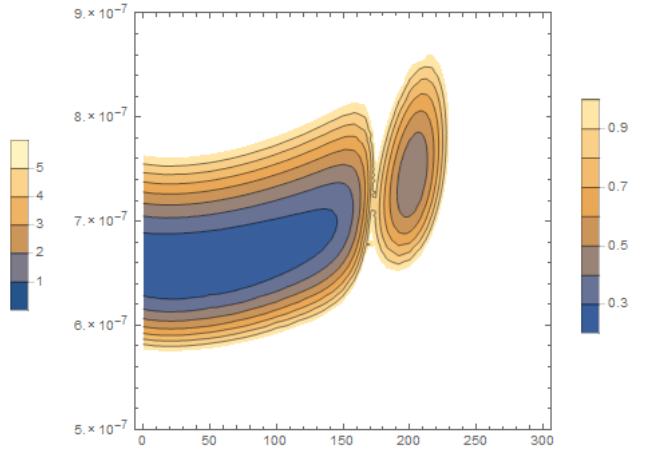
(c) ω fit

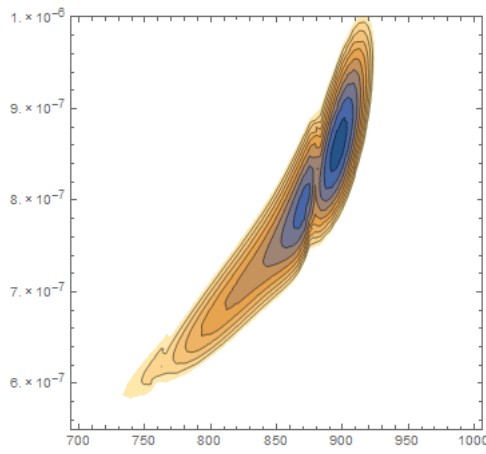(d) η fit
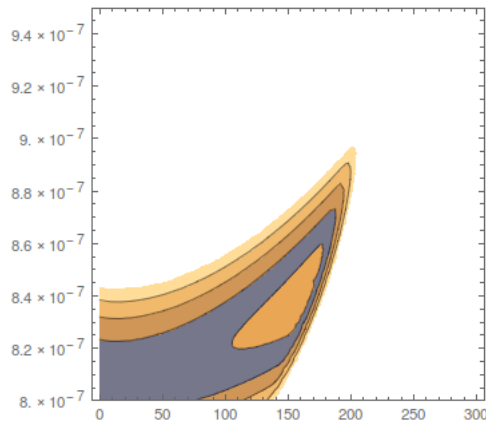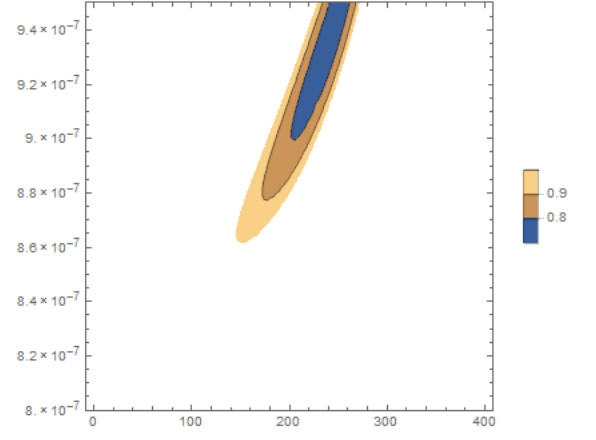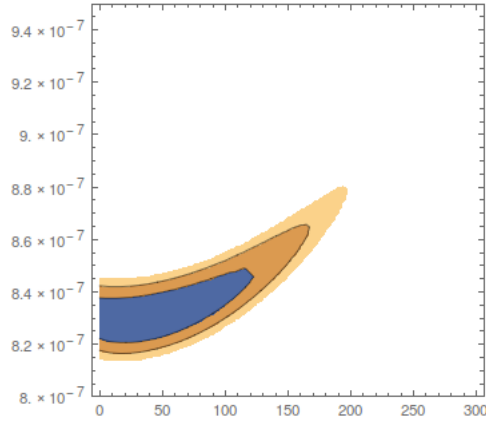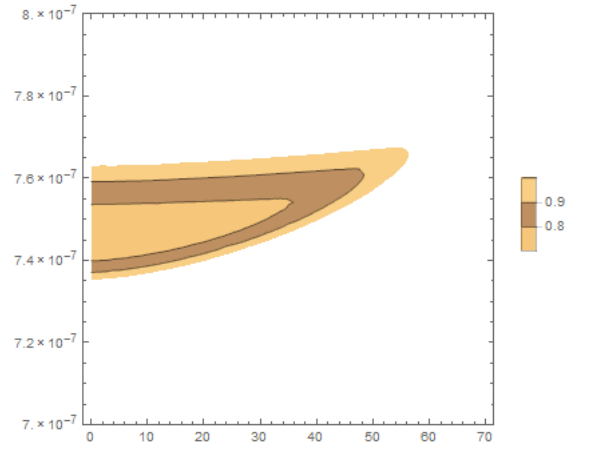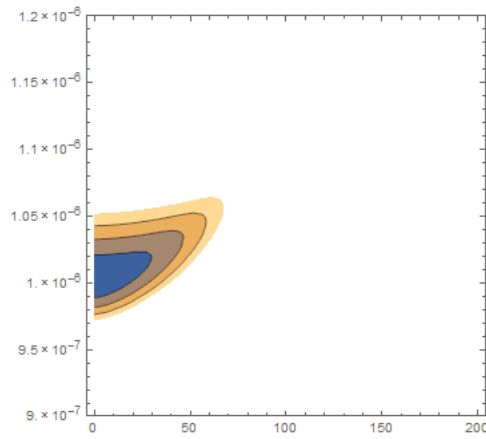
(e) a_0 fit
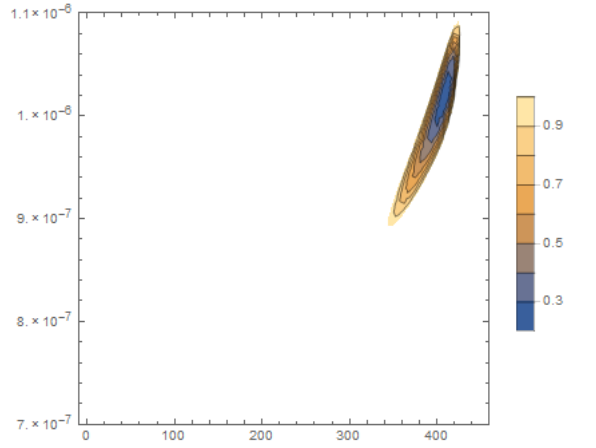
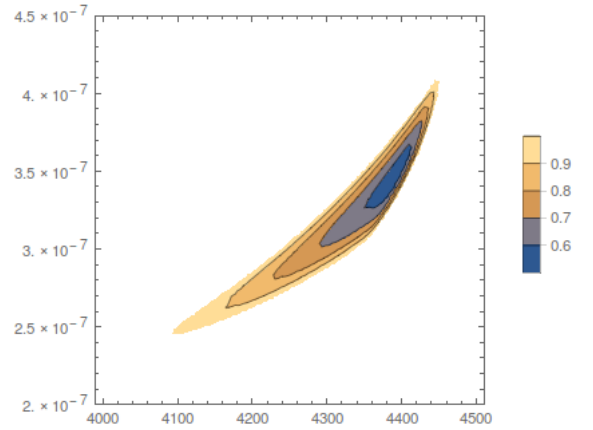(f) Φ fit

Figure 8: Symmetric Meson Fits
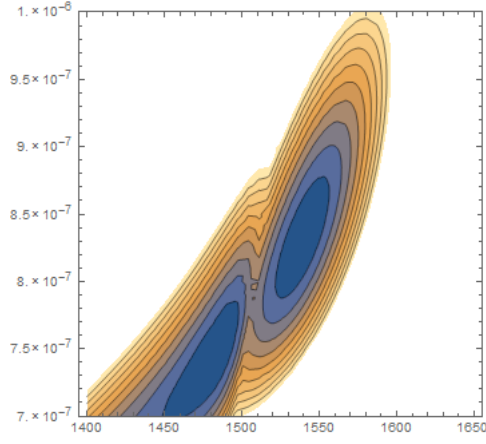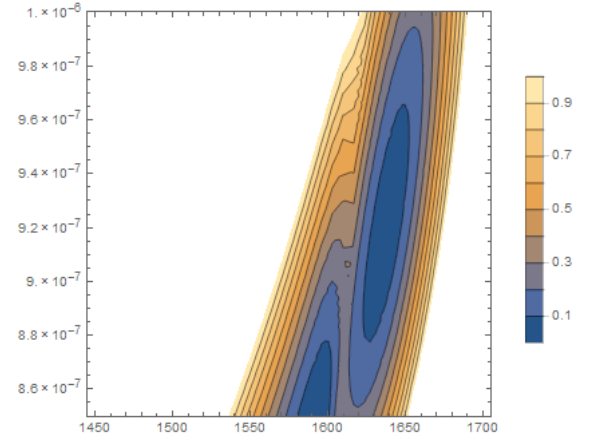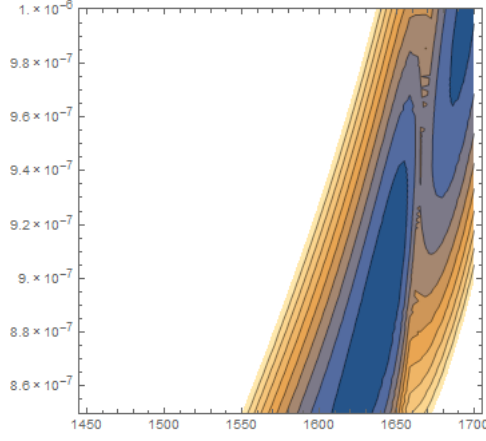
(a) K^* fit

(b) K fit

(c) D fit
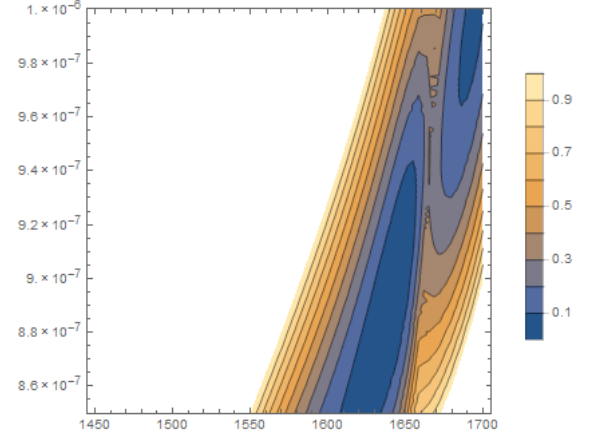
(d) Υ fit
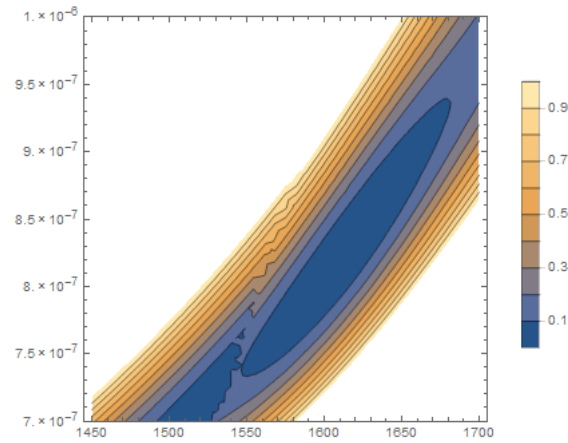
Figure 9: Symmetric Meson Fits

(a) $m_c = 250 MeV$ fit

(b) $m_c = 150 MeV$ fit

(c) $m_c = 100 MeV$ fit

(d) $m_c = 50 MeV$ fit
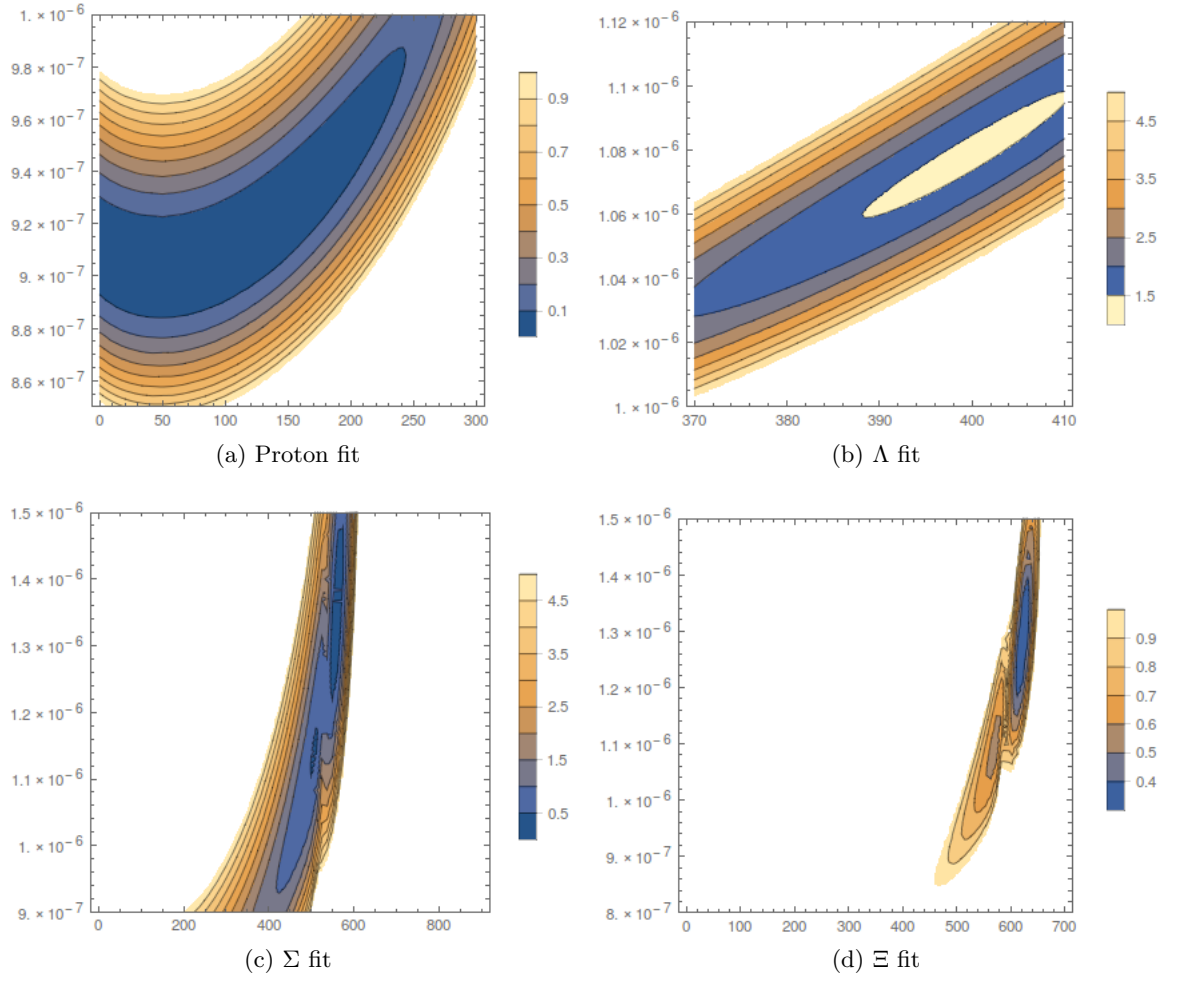
(e) $m_c = 5 MeV$ fit

Figure 10: Asymmetric D Meson Fits

(a) Proton fit

(b) Λ fit

(c) Σ fit

(d) Ξ fit

Figure 11: Baryon Fits

Hadron	$\alpha' \left[Gev^{-2}\right]$	Endpoint Masses[MeV]
π	0.82-0.86	100-170
ρ	0.86-1	150-300
ω	0.82-0.867	0-167
η	0.735-0.765	0-60
a_0	0.97-1.06	0-67
Φ	0.89-1.09	345-425
κ	> 0.845	> 218
K	0.57-0.86	0-228
D	0.58-1	733-923
D	0.86	$m_u = 150,\ m_c = 1594$
Υ	0.24-0.4	4095-4450

Table 3: Meson Fits Summary Table. The fit is symmetric unless endpoint masses indicate different endpoint masses.

Hadron	$\alpha' \left[Gev^{-2}\right]$	Endpoint Masses[MeV]
π	0.808-0.863	90-185
ρ	0.883-0.933	0-180
ω	0.910-0.918	0-60
η	0.839-0.854	0-70
Φ	1.078	400
κ	0.848-0.927	$m_{u/d} = 0 - 240\ m_s = 0 - 390$
D	1.073	$m_{u/d} = 80\ m_c = 1640$
Υ	0.635	4730

Table 4: Corresponding Meson Fits In [13]

Hadron	$\alpha' \left[Gev^{-2}\right]$	Endpoint Masses[MeV]
Proton	0.85-1	0-300
Λ	1.067-1.09	395-408
Σ	0.9-1.5	200-609
Ξ	0.847-1.5	459-657

Table 5: Baryon Fits Summary Table. Endpoint mass is the same on both endpoints.

Hadron	$\alpha' \left[Gev^{-2}\right]$	Endpoint Masses[MeV]
Proton	0.944-0.959	0-85
Λ	0.946-0.955	0-62.5
Σ	1.502	595
Ξ	1.455	660

Table 6: Corresponding Baryon Fits In [14]

3.2 The Mass Differences

We have calculated the mass differences as explained in section 2.8. Note that the formula used is 96 which does not contain any approximation. The results are shown in figure 12, having taken account of the uncertainty in the hadron masses by adding (subtracting) it to the maximum (minimum) value of the mass difference. The data used is shown in table 7. The states which were chosen could be identified as $J_{orbital} = 0$.

As explained in 2.8 the goal of the calculation requires obtaining a consistent value of the quark mass differences. However, inspecting 12 it is clear that the values thus obtained are not consistent. The most inconsistent values are those obtained from the K^* and D, while the values for the rest are fairly consistent.

The inconsistency for the K^* is made even more clear by figure 13 which compares the possible m_u/m_d quark mass differences as a function of the casimir coefficient a (the "intercept"), for the Kaon and the neutron/proton. Here it is evident that for most values of the intercept, the obtained mass differences are not consistent. In our case the values (shown in table 7 and taken from the Regge fits as previously mentioned) for "a" do not allow for a consistency even if some variation from them is allowed.

The mass difference calculated from the symmetric fit to the D trajectory turns out to be negative which is also not consistent with other calculations. We have tried using parameters from both a symmetric and a non symmetric fit to the D trajectory. The results are displayed in table 9. It seems that allowing for asymmetric masses can improve the situation in the quark mass difference calculation but cannot bring the mass difference to a positive value.

We have not been able to find a mechanism to bring the predicted quark mass differences in agreement. On the other hand it seems that a mass difference of $md - mu = 2.1 MeV$ is consistent for the hadrons composed of light quarks.

Taking this mass difference as input (also see tables 3,5), we can make a prediction of the mass differences of states with higher spin. This is done by calculating the energy of, say, a neutron and a proton at some angular momentum and subtracting. The difference in energy of course coming from the different quark masses and charges. Some values are in table 8.

Hadron	α'	Hadron Mass $[MeV]$	$|q_1 q_2|$	$\tilde{a}$	S
Proton	0.94	938.272	$\frac{2}{9}$	{-0.9,-0.31}	$\frac{1}{2}$
Neutron	0.94	939.565	$-\frac{1}{9}$	{-0.9,-0.31}	$\frac{1}{2}$
K^{*+}	0.86	889.11	$\frac{2}{9}$	{-0.27,-0.17}	1
K^{*0}	0.86	895.81	$-\frac{1}{9}$	{-0.27,-0.17}	1
Σ^+	0.95	1189.3	$\frac{2}{9}$	$\{-0.19, -0.12\}$	$\frac{1}{2}$
Σ^-	0.95	1197.449	$\frac{2}{9}$	$\{-0.19, -0.12\}$	$\frac{1}{2}$
Ξ^0	0.94	1314.86	$-\frac{1}{9}$	$\{-0.18, -0.03\}$	$\frac{1}{2}$
Ξ^-	0.94	1321.71	$\frac{2}{9}$	$\{-0.18, -0.03\}$	$\frac{1}{2}$
D^0 symmetric fit	0.86	1864.84	$-\frac{4}{9}$	$\{-0.012, 0\}$	0
D^+ symmetric fit	0.86	1869.61	$\frac{2}{9}$	$\{-0.012, 0\}$	0
D^0 asymmetric fit	0.86	1864.84	$-\frac{4}{9}$	$\{-0.022, -0.012\}$	0
D^+ asymmetric fit	0.86	1869.61	$\frac{2}{9}$	$\{-0.022, -0.012\}$	0

Table 7: Slope, Hadron masses, quark charges and casimir values used in the calculation of the mass differences. Casimir value pairs correspond to values taken for lower and upper limit for mass differences.

Mass Difference$[MeV]$			
Hadron	L=1	L=2	L=3
$M_{Proton} - M_{neutron}$	0.85	0.76	0.72
$M_{\Sigma^0} - M_{\Sigma^+}$	0.37	0.47	0.50
$M_{K^{*n}} - M_{K^{*+}}$	0.35	0.465	0.50

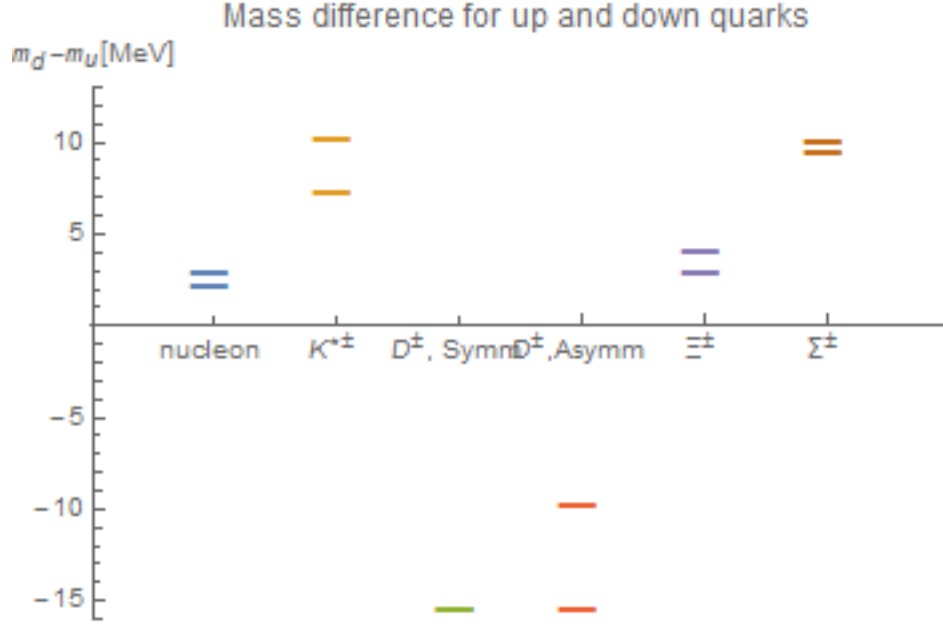Table 8: Projected mass differences for hadrons.

Figure 12: Mass differences between down and up quarks, calculated from various hadrons. For each hadron two values are calculated, each from a different possible value of the casimir term (consistent with the regge fits).
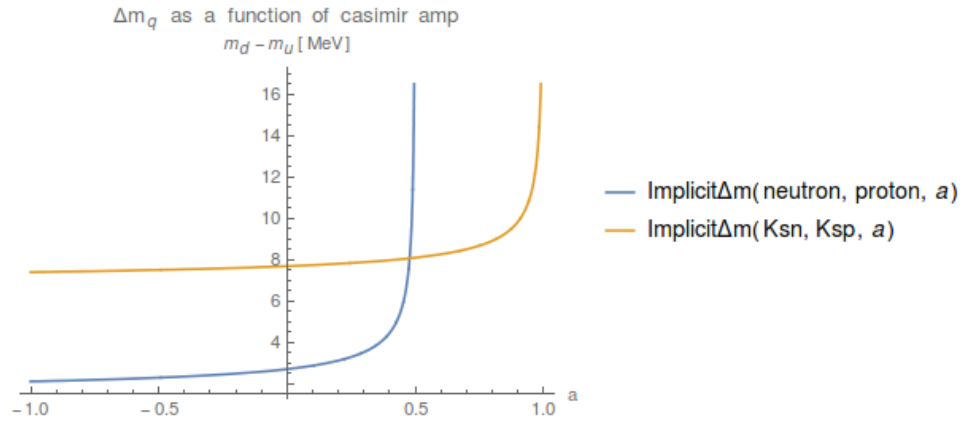

Figure 13: Mass differences between down and up quarks, calculated from $K^{*\pm}$ vs Proton/Neutron as a function of the "intercept" a.

u Mass[MeV]	$\alpha'[GeV^{-2}]$	charm Mass[MeV]	$\tilde{a}$	$m_d - m_u$[MeV]	$\frac{\chi_m^2}{\chi_l^2}$
250	0.45	1100	-0.18	-1.91596	0.729883
250	0.45	1185	-0.12	-3.6112	0.877145
250	0.86	1499	-0.01	-14.8343	0.875704
250	0.86	1548	0	-29.92	0.045734
250	0.86	1583	0	-29.91	0.943584
150	0.9	1568	-0.03	-6.59646	0.957694
150	0.9	1633	0	-29.15	0.0726242
150	0.9	1668	0	-29.1	0.862301
150	0.86	1544	-0.04	-5.30454	0.966513
150	0.86	1594	-0.01	-15.0193	0.0329892
100	0.86	1560	-0.06	-3.82673	0.915026
100	0.86	1628	-0.02	-9.96614	0.0435475
100	0.86	1677	0	-29.9	0.920127
100	0.9	1585	-0.05	-4.42282	0.941341
100	0.9	1699	0	-29.13	0.945629
50	0.86	1594	-0.06	-3.45495	0.366566
50	0.86	1594	-0.06	-3.45495	0.366566
50	0.9	1594	-0.07	-3.02502	0.923992
50	0.9	1594	-0.07	-3.02502	0.923992
5	0.7	1450	-0.19	-0.575249	0.638414
5	0.7	1578	-0.07	-3.85187	0.889484
5	0.86	1569	-0.11	-1.34976	0.895545
5	0.86	1695	-0.03	-6.88527	0.935499

Table 9: Fits of D meson and up/down quark mass differences for various choices of parameters.

4   Conclusions

In this thesis we have explored the properties of the string with massive and charged ends which corresponds holographically to hadrons. The casimir energy which is generated by quantum fluctuations of the string induces a repulsive force which keeps the string from collapsing in the case of attractive charges. The casimir energy together with the electromagnetic interaction is responsible for the Regge intercept. The repulsive nature of the casimir term is manifested as the constraint $\tilde{a} < 0$. This is also motivated by considering a zero spin state obeying linear trajectories which gives $J = \alpha' M^2 + \tilde{a} = 0$ so that $\tilde{a} = -\alpha' M^2 < 0$.

The resulting model was confronted with PDG data and the model parameters extracted for various hadrons. A new calculation which was attempted is the determination of the u/d mass difference. A mass difference between the u/d quarks exists in the range of $(-15) - 10 MeV$. The inconsistency is most prevalent when considering hadrons containing more massive quarks such as the **D** and κ mesons.

We suspect the inconsistencies in the calculated u/d mass difference is due to the system having some more unusual behaviour in the asymmetric masses case. As can be seen from the analysis in section 2.4.2, further research is needed to find a better solution of the charged system in the asymmetric case. This could change the results of the Regge trajectories in the asymmetric case and through the change in the parameters also change the mass difference results. Hopefully making all the mass differences consistent. The main difficulty in this direction is the complexity of the underlying equations. One option could be to find a numeric solution to the full equations of motion, but we have not been able to do this to date. Another option would be to perturbatively solve the equations, taking $q_1 q_2$ as the small parameter. This is left for future work and is beyond the scope of this thesis.

In conclusion, we get similar parameters for the Regge trajectory fits and we can determine the u/d quark mass difference. It should be emphasised the mass parameters in our model, as well as their differences, are not constituent quark model masses or current masses. Future research would address determining more precisely the electromagnetic radiation width relative to the strong interaction width, incorporating leptons into the model and incorporating the weak interaction into the model.

A   Conventions

The convention for the metric tensor is the same as in J. D. Jackson 3rd edition (equation 11.59, 11.81):

$$g_{\mu\nu} = sig(+, -, -, -)$$

And for the electromagnetic field tensor (equations 11.136, 11.137, 11.138):

$$F^{\alpha\beta} = \begin{pmatrix} 0 & -E_1 & -E_2 & -E_3 \\ E_1 & 0 & -B_3 & B_2 \\ E_2 & B_3 & 0 & -B_1 \\ E_3 & -B_2 & B_1 & 0 \end{pmatrix}$$

$$F_{\alpha\beta} = \begin{pmatrix} 0 & E_1 & E_2 & E_3 \\ -E_1 & 0 & -B_3 & B_2 \\ -E_2 & B_3 & 0 & -B_1 \\ -E_3 & -B_2 & B_1 & 0 \end{pmatrix}$$

B   Calculation of the Emitted Radiation

All excited hadron states are unstable, decaying either strongly, weakly or electromagnetically as can be seen by the decay products. In the main text we assumed the hadron to be electromagnetically stable, which implies that the radiated energy is negligible and that the angular component of the boundary equations can be ignored. This section describes the calculation of the radiated energy which can be made in two ways: a quantum mechanical calculation and a classical calculation.

B.1   Classical Calculation

We can calculate classically the amount of energy which is radiated out of the hadron as electromagnetic radiation. If the emitted energy is too large relative to the hadron mass, the hadron cannot be regarded as electromagnetically stable and our assumption of a steady state is invalid.

By a straightforward calculation of the power radiated by two rotating point charges one obtains

$$P = \alpha\omega^2\Pi(\beta) \tag{103}$$

Where α is the fine structure constant, ω is the rotation frequency and $\Pi(\beta)$ is a β dependent factor which diverges at $\beta = 1$. Figure 14 is a plot of $\Pi(\beta)$. Using relation 46 the radiated power is expressed as

$$P = \frac{\alpha T^2}{m_q^2\gamma^4\beta^2}\Pi(\beta) \tag{104}$$

Dividing the radiated power by the hadronic width gives us the total energy radiated over the hadrons' lifetime

$$E_{radiated} = \frac{\alpha T^2}{m_q^2\gamma^4\beta^2\Gamma_{hadron}}\Pi(\beta) \tag{105}$$

In the case of hadrons containing light quarks it is clear that most of the energy will be radiated by light quarks so we plug in the mass of the lightest
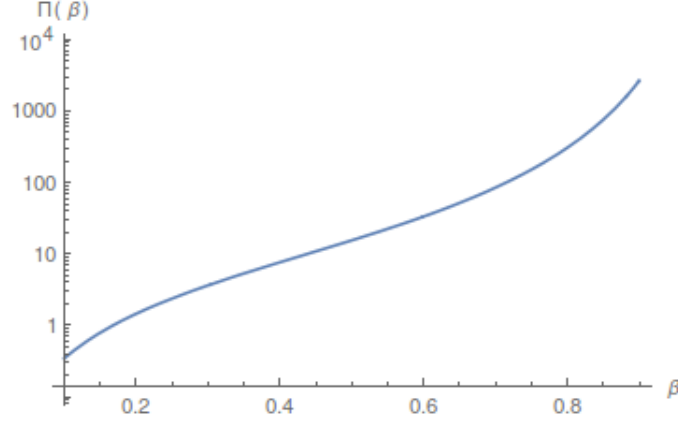
Figure 14: Envelope of the classical radiation

quark (or diquark) in the hadron, typically $m_q \simeq 130MeV$. In order to get a lower bound for the radiated energy we take $\beta = 0.7$ (a characteristic value in the Regge fits),$\Pi(0.7) \simeq 100$, $T = 0.17GeV^2$, $\alpha = \frac{1}{137}$ and $\Gamma_{hadron} = 200MeV$. We get

$$E_{radiated} \simeq 3312MeV \qquad (106)$$

Which is clearly far too large.

In the case of charmonium we have $m_q \simeq 1000MeV$ and $\Gamma_{\eta_c} = 28MeV$ so we have

$$E_{radiated} \simeq 400MeV \qquad (107)$$

Which is better but still 20% of the hadron's mass which is too large. We see that the classical calculation fails us. Luckily the quantum mechanical result is much more encouraging.

B.2   Quantum Mechanical Calculation

Quantum mechanically we compare the decay width of the hadron with the decay width of the electromagnetic decay channel. If the electromagnetic decay rate is negligible compared with the hadron decay rate, the probability for electromagnetic decay must be negligible. The decay width can be computed using Fermi's golden rule and the dipole approximation, obtaining (in natural units):[27]

$$\Gamma = \frac{4\alpha\Delta E^3|\langle 1|\mathbf{r}|2\rangle|^2}{3} \qquad (108)$$

Where ΔE is the energy difference between the initial and final "atomic" energy levels. We use here the energy difference between two electromagnetic energy levels in the hadron which we can estimate by using the hydrogen atom relation:

$$E_n = -\frac{m_q\alpha^2}{2n^2} \qquad (109)$$

So that the maximal energy difference between two electromagnetic levels is:

$$\Delta E = \frac{m_q \alpha^2}{2} \tag{110}$$

The formula for the width also involves a non-perturbative matrix element. It can be calculated in the potential model formalism (see section 1.6) but we don't know of an existing result. By dimensional analysis it should be proportional to the string length.

$$\langle 1|\mathbf{r}|2\rangle \sim l \simeq \frac{2\beta}{\omega} \simeq \frac{2m_q \gamma^2 \beta^2}{T} \tag{111}$$

where relation 46 was used. Putting everything together we have

$$\Gamma = \frac{2\alpha^7 m_q^5 \gamma^4 \beta^4}{3T^2} \tag{112}$$

Finally, we can estimate an upper bound for the width of decay from one electromagnetic energy level to another by taking $\alpha = \frac{1}{137}$, $m_q = 1.5 GeV$, $T = 0.17 GeV^2$, $\beta = 0.99$ and get

$$\Gamma \simeq 4.6 \times 10^{-7} MeV \tag{113}$$

By noting that $\Gamma_{hadron} > 1 MeV$, this indicates

$$\frac{\tau_{hadron}}{\tau_{electromagnetic}} = \frac{\Gamma_{electromagnetic}}{\Gamma_{hadron}} \lesssim 4.6 \times 10^{-7} \tag{114}$$

Which tells us that the probability for the hadron to experience any electromagnetic decay during its' lifetime is negligible, making it effectively electromagnetically stable.

C   Taking The Nonrelativistic Limit

In this appendix I will show the manner of taking the nonrelativistic limit in order to arrive at equations 94.

We start out from equations 98, taking the limit $\beta_1 \to 0$. We need to determine the β_1 dependence of the quantities $\beta_2, \Delta\theta$ and $\sin(\Delta\theta)$.

Determining β_2 is done using using equation 86. The form for β_2 is $\beta_2 = a_0 + a_1\beta_1 + O(\beta^3)$. Replacing into the equation results in a power series in β_1 which is equated to zero, so that each coefficient in the series must vanish. This gives equations for the coefficients $(a_0, a_1, ...)$ with the result

$$\beta_2 = \frac{m_1}{m_2}\beta_1 + O(\beta_1^3)$$

Mathematica code for the computation of β_2:

```
eq = m1 β1/(1 - β1²) - m2 β2/(1 - β2²);
β2 = SeriesData[β1, 0, {a1, a2, a3}, 1, 3, 1]
solβ2 = Solve[eq == 0, {a1, a1, a2}][[1]]
```

Using the same method we compute $\Delta\theta$ from equation 72. We put in the solution for β_2 and get

$$\Delta\theta = \frac{m_1 + m_2}{m_2}\beta_1 + O\left(\beta_1^2\right)$$

The solution of $\sin(\Delta\theta)$ relevant to us is immediate by noting that for $\Delta\theta \to 0$, $\Delta\theta \approx \sin(\Delta\theta)$.

Mathematica code for the computation of $\Delta\theta$:

```
eqret = φ² - β1² - β2² - 2 β1 β2 Cos[φ] /. solβ2;
φ = SeriesData[β1, 0, {b1, b2, b3}, 1, 4, 1]
solφ = Solve[eqret == 0, {b1, b2}][[2]]
```

The final step in obtaining equations 94 is expanding equations 98 in a taylor series using the two previous results. Mathematica code for the expansion of the energy and force equation:

```
ω = (β1 + β2)/(l1 + l2) /. solβ2

En =

( T/ω (ArcSin[β1] + ArcSin[β2]) + m1/√(1 - β1²) + m2/√(1 - β2²) + q1 q2 ω/(β1 β2 Sin[φ] + φ) - π/2 (a - S) ω/(β1 + β2) ) /.

solβ2 /. solφ

-T √(1 - β1²) + m2 β1 ω/√(1 - β1²) -

(q1 q2 ω² (-2 β1 + β1 β2² + 2 β2 (-1 + β2²) Cos[φ] + β1 β2² Cos[2 φ] - 2 β2 φ Sin[φ])) /
  (2 (φ + β1 β2 Sin[φ])³) +
(q1 q2 β1 β2 ω² (β1 (1 + β2²) φ Cos[φ] + β1 (β1² + β2²) Sin[φ] +

  β2 (φ + β1² φ + β1² Sin[2 φ]))) / (φ (φ + β1 β2 Sin[φ])³) - π (a - S) ω²/(2 (β1 + β2)²) /. solβ2 /.

solφ
```

This results in the expressions:

$$E = -\frac{\pi}{2}\frac{\tilde{a}}{l_1 + l_2} + \frac{q_1 q_2}{l_1 + l_2} + T(l_1 + l_2) + m_1 + m_2 \tag{115a}$$

$$J = 0 \tag{115b}$$

$$\frac{q_1 q_2}{(l_1 + l_2)^2} - \frac{\pi}{2}\frac{\tilde{a}}{(l_1 + l_2)^2} = T \tag{115c}$$

Which is what we expected.

D   Obtaining Analytic Trajectories

D.1   Relativistic Limit

The code for obtaining $\beta_2\left(\beta_1\right)$ and $\Delta\theta\left(\beta_1\right)$ (here called θ):

```mathematica
order = 10;
β1 = Series[1 - ε^2, {ε, 0, order}];
β2 = SeriesData[ε, 0, Table[b[i], {i, 1, 2 order}], 0, 2 order, 1];
β2 = β2 /. Solve[β1 m1 β2^2 + β2 m2 (1 - β1^2) - β1 m1 == 0, Table[b[i], {i, 1, 2 order}]][[2]];
γ1 = (1 - β1^2)^(-1/2);
γ2 = (1 - β2^2)^(-1/2);
ϴ = SeriesData[ε, 0, Prepend[Table[a[i], {i, 2, order}], a[1]], 0, order, 1];
ϴeq = ϴ^2 - β1^2 - β2^2 - 2 β1 β2 Cos[ϴ];
a[1] = a[1] /. FindRoot[SeriesCoefficient[ϴeq, 0] == 0, {a[1], 1}];
ϴ = FullSimplify[ϴ /. Solve[ϴeq - SeriesCoefficient[ϴeq, 0] == 0, Table[a[i], {i, 2, order}]][[1]]];
```

Using that, the code for obtaining the trajectory is:

```mathematica
ω =
  Simplify[
   Series[
    ωω /.
     Solve[
       Normal[-T Sqrt[1 - β1^2] + (m1 β1 ωω)/Sqrt[1 - β1^2] -
        Rationalize[(q^2 ωω^2 (-2 β1 + β1 β2^2 + 2 β2 (-1 + β2^2) Cos[ϴ] + β1 β2^2 Cos[2 ϴ] - 2 β2 ϴ Sin[ϴ]))/(2 (ϴ + β1 β2 Sin[ϴ])^3) +
         (q^2 β1 β2 ωω^2 (β1 (1 + β2^2) ϴ Cos[ϴ] + β1 (β1^2 + β2^2) Sin[ϴ] + β2 (ϴ + β1^2 ϴ + β1^2 Sin[2 ϴ])))/(ϴ (ϴ + β1 β2 Sin[ϴ])^3), 10^-5] - π/2 (a - S) ωω^2/(β1 + β2)^2] ==
       0, ωω][[1]], {ε, 0, order}], ε > 0 && m1 > 0 && m2 > 0];
H = Simplify[T/ω (ArcSin[β1] + ArcSin[β2]) + (m1 γ1 + m2 γ2) + q^2 ω Rationalize[(1/(β1 β2 Sin[ϴ] + ϴ)), 10^-5] - π/2 (a - S) ω/(β1 + β2), ε > 0 && m1 > 0 && m2 > 0];
J = Simplify[T (-β1/γ1 + ArcSin[β1] - β2/γ2 + ArcSin[β2])/(2 ω^2) + m1 (γ1 β1^2)/ω + m2 (γ2 β2^2)/ω - 2 q^2 β1 β2 Rationalize[Cos[ϴ]/(β1 β2 Sin[ϴ] + ϴ), 10^-5], ε > 0 && m1 > 0 && m2 > 0];
ep = InverseSeries[H, En];
traj = FullSimplify[ComposeSeries[J, ep], {m1 > 0, m2 > 0}] /. {T → 1/(2 π α)};
```

D.2   Non Relativistic Limit

The code for obtaining $\beta_2\left(\beta_1\right)$ and $\Delta\theta\left(\beta_1\right)$ (here called θ):

```mathematica
order = 6;
β2 = Simplify[Series[β2 /. Solve[β1 m1 β2^2 + β2 m2 (1 - β1^2) - β1 m1 == 0, β2][[2]], {β1, 0, order}], m2 > 0];
γ1 = Series[(1 - β1^2)^(-1/2), {β1, 0, order}];
γ2 = (1 - β2^2)^(-1/2);
ϴ = SeriesData[β1, 0, Table[a[i], {i, order}], 1, order, 1];
ϴeq = ϴ^2 - β1^2 - β2^2 - 2 β1 β2 Cos[ϴ];
ϴ = FullSimplify[ϴ /. Solve[ϴeq == 0, Table[a[i], {i, 1, order}]]][[1]];
```

Using that, the code for obtaining the trajectory is:

```
ω =
  Simplify[
    Series[
      ωω /.
        Solve[Normal[-T √(1 - β1²) + (m1 β1 ωω)/√(1 - β1²) - (q² ωω² (-2 β1 + β1 β2² + 2 β2 (-1 + β2²) Cos[σ] + β1 β2² Cos[2 σ] - 2 β2 σ Sin[σ])) / (2 (σ + β1 β2 Sin[σ])³) +

          (q² β1 β2 ωω² (β1 (1 + β2²) σ Cos[σ] + β1 (β1² + β2²) Sin[σ] + β2 (σ + β1² σ + β1² Sin[2 σ]))) / (σ (σ + β1 β2 Sin[σ])³) - π/2 ((a - S) ωω²)/(β1 + β2)²] == 0, ωω][[

          1]], {β1, 0, order}], β1 > 0 && m1 > 0 && m2 > 0 && T > 0];
H = Simplify[T/ω (ArcSin[β1] + ArcSin[β2]) + (m1 γ1 + m2 γ2) + q² ω (1/(β1 β2 Sin[σ] + σ)) - π/2 ((a - S) ω)/(β1 + β2), β1 > 0 && m1 > 0 && m2 > 0 && T > 0];
J = Simplify[T (-β1/γ1 + ArcSin[β1] - β2/γ2 + ArcSin[β2])/(2 ω²) + m1 (γ1 β1²)/ω + m2 (γ2 β2²)/ω - 2 q² β1 β2 Cos[σ]/(β1 β2 Sin[σ] + σ), β1 > 0 && m1 > 0 && m2 > 0 && T > 0];
βp = InverseSeries[H, En];
traj = ComposeSeries[J, βp];
```

E   Mass Difference Code

This appendix documents the Mathematica code used for calculating the mass differences. The data is entered as:

```
keys = {proton, neutron, ρp, ρn, Ksp, Ksn, Σp, Σn, Ξn, Ξm, Dn, Dp};
Mass = <| proton → 938.27204, neutron → 939.56537, Ksp → 889.11, Ksn → 895.81, Ξcn → 2470.88, Ξcp → 2467.8, Λcp → 2286.46,
    Dn → 1864.84, Dp → 1869.61, πp → 139.57, πn → 134.97, Σcp → 2452.9, Σcn → 2453.74, Σp → 1189.3, Σn → 1192.6, ρn → 775.26,
    ρp → 775.96, Bn → 5279.61, Bp → 5279.29, Ξn → 1314.86, Ξm → 1321.71, Kn → 497.614, Kp → 493.677|>;
m1 = <| proton → mu, neutron → md, Ksp → ms, Ksn → ms, Ξcn → mc, Ξcp → mc, Λcp → md, Dp → md, Dn → mu, πp → mu, πn → (mu + md)/2,
    Σcp → mc, Σcn → mc, Σp → ms, Σn → ms, ρn → (mu + md)/2, ρp → mu, Bn → mb, Bp → mb, Ξn → ms, Ξm → ms, Kn → ms, Kp → ms|>;
m2 = <| proton → md, neutron → md, Ksp → mu, Ksn → md, Ξcn → md, Ξcp → mu, Λcp → mc, Dp → mc, Dn → mc, πp → md, πn → (mu + md)/2,
    Σcp → mu, Σcn → md, Σp → mu, Σn → md, ρn → (mu + md)/2, ρp → md, Bn → md, Bp → mu, Ξn → ms, Ξm → ms, Kn → md, Kp → mu |>;
Spin = <|Ksp → 1, Ksn → 1, proton → 1/2, neutron → 1/2, Ξcn → 1/2, Ξcp → 1/2, Λcp → 1/2, Dn → 1, Dp → 1, πp → 0, πn → 0, Σcp → 1/2,
    Ξcn → 1/2, Σp → 1/2, Σn → 1/2, ρn → 1, ρp → 1, Bn → 0, Bp → 0, Ξn → 1/2, Ξm → 1/2, Kn → 0, Kp → 0|>;
Q = <|Ksp → 2/9, Ksn → -1/9, proton → 2/9, neutron → -1/9, Λcp → 2/9, Dn → 4/9, Dp → 2/9, πp → 2/9, πn → -5/18, Σcp → 2/9, Σcn → -1/9,
    Σp → 2/9, Σn → -1/18, ρn → -5/18, ρp → 2/9, Bn → -1/9, Bp → 2/9, Ξn → -1/9, Ξm → 2/9, Kn → -1/9, Kp → 2/9|>;
α = <|Ksp → 0.96, Ksn → 0.96, proton → 0.94, neutron → 0.94, Λcp → 0.95, Dp → 0.86, Dn → 0.86, πp → 0.86, πn → 0.86, Σcn → 0.95,
    Σcp → 0.95, Σn → 0.95, Σp → 0.95, ρn → 0.86, ρp → 0.86, Bn → 0.86, Bp → 0.86, Ξn → .94, Ξm → .94, Kn → 0.86, Kp → 0.86|>;
(*for summup purposes*)
intercepts = <|Ksp → {0.9, 0.94}, Ksn → {0.9, 0.94}, proton → {-0.67, -0.15}, neutron → {-0.67, -0.15}, Dn → {0.86, 1},
    Dp → {0.86, 1}, Σp → {0.306487, 0.371938}, Σn → {0.306487, 0.371938}, ρn → {0.5, 0.9}, ρp → {0.5, 0.9}, Ξn → {0.316, 0.465},
    Ξm → {0.316, 0.465} |>;
```

The functions used for calculating the mass differences are:

$$M[key\_, a\_] := \sqrt{\frac{2}{\pi\, 10^{-6}\, \alpha[key]}}\, \sqrt{\frac{1}{137}\, Q[key] - (a - Spin[key])}\ ;$$

```
TotM[key_, a_] := M[key, a] + m1[key] + m2[key];
ImplicitΔm[key1_, key2_, a_] := Mass[key1] - Mass[key2] - M[key1, a] + M[key2, a];
Δmsq[key1_, key2_, a1_, a2_] := TotM[key1, a1]² - TotM[key2, a2]²;
```

The code for generating the results is:

```
(*Generate Graph of Mass Differences*)
ListPlot[{
  {1, ImplicitΔm[neutron, proton, -0.67] + 0.000021}, {1, ImplicitΔm[neutron, proton, -0.15] - 0.000021},
  {2, ImplicitΔm[ρn, ρp, 0.5] - 0.8}, {2, ImplicitΔm[ρn, ρp, 0.9] + 0.8},
  {3, ImplicitΔm[Ksn, Ksp, 0.9] - 1.2}, {3, ImplicitΔm[Ksn, Ksp, 0.94] + 1.2},
  {4, ImplicitΔm[Dp, Dn, 0.86] + 0.1}, {4, ImplicitΔm[Dp, Dn, 0.95] - 0.1},
  {5, ImplicitΔm[Ξm, Ξn, 0.316] - 0.024}, {5, ImplicitΔm[Ξm, Ξn, 0.465] + 0.024}, {6, ImplicitΔm[Ξn, Ξp, 0.306487] - 0.035},
  {6, ImplicitΔm[Ξn, Ξp, 0.371938] + 0.035}, {7, ImplicitΔm[Bn, Bp, -0.00001]}, {7, ImplicitΔm[Bn, Bp, -10^-8]}},
 PlotMarkers → {"-", 30}, AxesLabel → {"", "m_d-m_u[MeV]"},
 PlotLabel → "Mass difference for up and down quarks",
 Ticks → {{{1, "proton/neutron"}, {2, "ρ^±"}, {3, "K^*±"}, {4, "D^±"}, {5, "Ξ^±"}, {6, "Ξ^±"}}, Automatic}]

(*Generate Data Table*)
Grid[Prepend[Table[{keys[[i]], α[keys[[i]]], Mass[keys[[i]]], Q[keys[[i]]], intercepts[keys[[i]]] - Spin[keys[[i]]], Spin[keys[[i]]]},
   {i, Length[keys]}], {key, alpha, mass, q, a - S, S, Δmass}], Frame → All]
(*Generate Graph of Proton-Neutron vs K* mass differences*)
Plot[{ImplicitΔm[neutron, proton, a], ImplicitΔm[Ksn, Ksp, a]}, {a, -1, 1}, PlotLabel → "Δm_q as a function of casimir amp",
 PlotLegends → "Expressions", AxesLabel → {"a", "m_d-m_u[MeV]"}]
```

References

[1] P. Collins, *An Introduction to Regge Theory and High Energy Physics*, Cambridge University Press, 1977.

[2] Weisstein, Eric W, *Series Reversion*, From MathWorld–A Wolfram Web Resource, http://mathworld.wolfram.com/SeriesReversion.html

[3] J. Greensite, *The Confinement Problem in Lattice Gauge Theory*, Prog.Part.Nucl.Phys. 51 (2003) 1, arXiv:hep-lat/0301023v2, 2003.

[4] Wolfgang Lucha, Franz F. Schoberl and Dieter Gromes, *Bound States of Quarks*, PHYSICS REPORTS (Review Section of Physics Letters) 200, No. 4 (1991) 127-240, 1989.

[5] Juan Maldacena, *The Large N Limit of Superconformal Field Theories and Supergravity*, Adv.Theor.Math.Phys.2:231-252,1998, arXiv:hep-th/9711200v3, 1997.

[6] Edward Witten, *Anti-de Sitter Space, Thermal Phase Transition, And Confinement In Gauge Theories*, Adv.Theor.Math.Phys.2:505-532,1998, arXiv:hep-th/9803131v2, 1998.

[7] S. Kuperstein, J. Sonnenschein, *Non-critical, near extremal AdS6 background as a holographic laboratory of four dimensional YM theory*, JHEP0411:026,2004, arXiv:hep-th/0411009v1, 2004.

[8] Ofer Aharony, Steven S. Gubser, Juan Maldacena, Hirosi Ooguri and Yaron Oz, *Large N Field Theories, String Theory and Gravity*, Phys.Rept.323:183-386,2000, hep-th/9905111, 2011.

[9] Paolo Di Vecchia, *An introduction to AdS/CFT equivalence*, Fortsch.Phys.48:87-92,2000, arXiv:hep-th/9903007v1, 1998.

[10] Juan Maldacena, *Wilson loops in large N field theories*, Phys.Rev.Lett. 80 (1998) 4859-4862, arXiv:hep-th/9803002v3, 1998.

[11] S.S. Gubser, I.R. Klebanov, A.M. Polyakov, *Gauge Theory Correlators from Non-Critical String Theory*, Phys.Lett.B428:105-114,1998, arXiv:hep-th/9802109v2, 1998.

[12] Jacob Sonnenschein, *Stringy Confining Wilson Loops*, Contribution to the Proceedings of the TMR Conference "Non-Perturbative Quantum Effects 2000," Paris, September 2000, arXiv:hep-th/0009146v1, 2000.

[13] Jacob Sonnenschein, Dorin Weissman, *Rotating strings confronting PDG mesons*, JHEP 1408 (2014) 013, arXiv:1402.5603v3, 2014.

[14] Jacob Sonnenschein, Dorin Weissman, *A rotating string model versus baryon spectra*, JHEP 1502 (2015) 147, arXiv:1408.0763v3, 2015.

[15] J. Polchinski and A. Strominger, *Effective string theory*, Phys.Rev.Lett. 67 (1991) 16811684, 1991.

[16] S. Hellerman and I. Swanson, *String Theory of the Regge Intercept*, arXiv:1312.0999, 2013.

[17] S. Hellerman, S. Maeda, J. Maltz and I. Swanson, Effective String Theory Simplified, JHEP 1409, 183 (2014) doi:10.1007/JHEP09(2014)183 [arXiv:1405.6197 [hep-th]]

[18] G. Lambiase and V. V. Nesterenko, *Quark mass correction to the string potential*, Phys.Rev. D54 (1996) 6387-639, 1996.

[19] Y. Kinar, E. Schreiber, J. Sonnenschein, *$Q\bar{Q}$ Potential from Strings in Curved Spacetime - Classical Results*, Nucl.Phys. B566 (2000) 103-125, arXiv:hep-th/9811192v1, 1998.

[20] Y. Kinar, E. Schreiber, J. Sonnenschein, N. Weiss, *Quantum fluctuations of Wilson loops from string models*, Nucl.Phys. B583 (2000) 76-104, arXiv:hep-th/9911123v2, 1999.

[21] Martin Kruczenski, Leopoldo A. Pando Zayas, J. Sonnenschein, Diana Vaman, *Regge Trajectories for Mesons in the Holographic Dual of Large-N_c QCD*, JHEP0506:046,2005, arXiv:hep-th/0410035v2, 2005.

[22] J.D. Jackson, *Classical Electrodynamics 3rd edition*, Wiley, 1998.

[23] K.A. Olive et al. (Particle Data Group), *The Review of Particle Physics*, Chin. Phys. C, 38, 090001 (2014), 2015 update.

[24] A.V. Manohar and C.T. Sachrajda, *Quark Masses*, http://pdg.lbl.gov/2015/reviews/rpp2014-rev-quark-masses.pdf, 2014 update.

[25] Tadakatsu Sakai, Shigeki Sugimoto, *Low energy hadron physics in holographic QCD*, Prog.Theor.Phys.113:843-882,2005, arXiv:hep-th/0412141v5, 2004.

[26] Shigenori Seki, Jacob Sonnenschein, *Comments on Baryons in Holographic QCD*, JHEP 0901:053,2009, arXiv:0810.1633v3, 2008.

[27] Marian O Scully, M. Suhail Zubairy, *Quantum optics*, eq. 6.3.14 pp. 206-207, Cambridge University Press, 1997.